

AD-757 086

Plasma Cathode for E-Beam Lasers

Hughes Research Laboratories

**prepared for
Advanced Research Projects Agency**

NOVEMBER 1972

Distributed By:

NTIS

**National Technical Information Service
U. S. DEPARTMENT OF COMMERCE**

AD 757028

Reproduced by
NATIONAL TECHNICAL
INFORMATION SERVICE
U S Department of Commerce
Springfield VA 22151



SEMIANNUAL TECHNICAL REPORT
CONTRACT NUMBER 72-0-040



PLASMA CATHODE FOR E-BEAM LASERS

1 MAY 1972 THROUGH 30 NOVEMBER 1972



DOCUMENT CONTROL DATA - R&D

(Security classification of title, body of abstract and indexing annotation must be entered when the overall report is classified)

1. ORIGINATING ACTIVITY (Corporate author) Hughes Research Laboratories 3011 Malibu Canyon Road Malibu, CA 90265		2a. REPORT SECURITY CLASSIFICATION Unclassified	
		2b. GROUP N/A	
3. REPORT TITLE PLASMA CATHODE FOR E-BEAM LASERS			
4. DESCRIPTIVE NOTES (Type of report and inclusive dates) Semiannual Technical Report, 1 May 1972 through 30 Nov. 1972			
5. AUTHOR(S) (First name, middle initial, last name) R.C. Knechtli and G.N. Mercer			
6. REPORT DATE February 1973		7a. TOTAL NO. OF PAGES 70 72	7b. NO. OF REFS 9
8a. CONTRACT OR GRANT NO. N00014-72-C-0496		9a. ORIGINATOR'S REPORT NUMBER(S)	
b. PROJECT, TASK, WORK UNIT NOS.			
c. DOD ELEMENT		9b. OTHER REPORT NO(S) (Any other numbers that may be assigned this report)	
d. DOD SUBELEMENT			
10. DISTRIBUTION STATEMENT Distribution of this document is unlimited.			
11. SUPPLEMENTARY NOTES Details of illustrations in this document may be better studied on microfiche		12. SPONSORING MILITARY ACTIVITY Advanced Research Projects Agency Arlington, VA 22209	
13. ABSTRACT <p>The technical goal of this program is to develop a superior substitute for the thermionic-cathode electron gun used for plasma conditioning in high energy lasers. Specifically, the program is directed toward developing a hollow cathode plasma electron source to replace the thermionic source commonly used in these electron guns.</p> <p>To fulfill the technical goals of the program, a theoretical and experimental development program is being carried out. A small scale prototype of the plasma cathode electron gun has been constructed and tested with excellent results. A high-voltage, full-size module is now under construction.</p> <p>The results obtained to date have verified the general theory of operation of the plasma cathode electron gun. They have established the feasibility of a high voltage gun operating with beam pulse durations of 1 μsec to 1 msec and beam current densities up to 50 A/cm².</p> <p>These results indicate that electron guns for high energy e-beam lasers can be constructed which are simpler, more efficient, and more rugged than the present guns. The new guns will simplify the construction and operation of high energy lasers. Work is continuing on expanding the beam dimensions of the plasma cathode e-gun. The high-voltage module now under construction will produce a beam 1 cm x 13 cm. Side-by-side stacking of the basic module will permit the production of very large-area beams.</p>			

HUGHES RESEARCH LABORATORIES
Malibu, California

a division of hughes aircraft company

PLASMA CATHODE FOR E-BEAM LASERS

Semiannual Technical Report
N00014-72-C-0496
1 May 1972 through 30 November 1972

ARPA Order No. 1807
Program Code No. 2E20

Amount of Contract: \$79,484.00
Principal Investigator: R.C. Knechtli
(213)456-6411
Principal Scientist: G.N. Mercer

This research was supported by the Advanced Research Projects Agency of the Department of Defense and was monitored by ONR under Contract N00014-72-C-0496.

Reproduction in whole or in part is permitted for any purpose of the United States Government.

TABLE OF CONTENTS

I	INTRODUCTION	1
	A. Objectives	1
	B. Technical Approach	3
	C. Program Organization	9
II	LOW PRESSURE DISCHARGE PLASMA SOURCE	8
	A. General	13
	B. Crossed Field Discharge	21
	C. Hollow Cathode Discharge	32
III	ELECTRON EXTRACTION	43
	A. Theoretical Guidelines	43
	B. Experimental Results	45
IV	PASCHEN BREAKDOWN	53
	A. Effect of High Voltage Electron Beam on Breakdown Characteristics	53
V	DESIGN OF HIGH VOLTAGE PLASMA CATHODE ELECTRON GUN	59
	A. Basic Design Parameters	59
	B. Design of Rectangular Gun	61
VI	CONCLUSIONS AND FUTURE PLANS	65
	REFERENCES	67

LIST OF ILLUSTRATIONS

1	Plasma cathode electron gun concept	4
2	Paschen breakdown in helium	6
3	Low pressure breakdown characteristics	8
4	Plasma cathode electron gun schematic	10
5	Crossed-field discharge device	14
6	Hollow cathode discharge ignition test vehicle	16
7	Low voltage plasma cathode E-gun device	17
8	Cathode and crossed-field tube anode	18
9	Anode feedthrough design of experimental tube . . .	20
10	Electron and ion paths in a coaxial cylindrical crossed-field geometry	23
11	Qualitative potential distribution in crossed-field tube	25
12	Crossed-field tube voltage-current characteristics, $p = 100$ mTorr	29
13	Crossed-field tube voltage-current characteristics, $p = 75$ mTorr	29
14	Crossed-field tube voltage-current characteristics, $p = 50$ mTorr	30
15	Crossed-field tube voltage-current characteristics, $p = 35$ mTorr	30
16	Crossed-field tube voltage-current characteristics, $p = 30$ mTorr	30
17	Crossed-field tube voltage as a function of gas pressure with $B = 240$ g and $I = 0.6$ A	31
18	Hollow cathode discharge configuration	33

19	Hollow cathode tube voltage-current characteristics	38
20	Expanded view of electron extraction from plasma	44
21	Cylindrical electron extractor	46
22	Elements of cylindrical extractor assembly	47
23	Low voltage electron extraction characteristics	49
24	Qualitative behavior of Paschen breakdown voltage as a function of pressure x electron spacing	54
25	Assembly for study of Paschen breakdown in the presence of E-beam	57
26	Operating point of high-voltage rectangular gun in relation to vacuum and Paschen breakdown	60
27	Artist's drawing of high voltage plasma cathode electron gun without corona shielding	62
28	Ceramic vacuum envelope and insulator for high-voltage rectangular gun	63
29	Cross-sectional schematic of high- voltage rectangular gun	64

SUMMARY

The technical goal of this program is to develop a superior substitute for the thermionic-cathode electron gun used for plasma conditioning in high energy lasers. Specifically, the program is directed toward developing a hollow cathode plasma electron source to replace the thermionic source commonly used in these electron guns. The general technical approach is outlined in Section I-B.

To fulfill the technical goals of the program, a theoretical and experimental development program is being carried out. A small-scale prototype of the plasma cathode electron gun has been constructed and tested with excellent results. A high-voltage, full-size module is now under construction. Its design parameters are given in Section V-B.

The results obtained to date have verified the general theory of operation of the plasma cathode electron gun. They have established the feasibility of a high voltage gun operating with beam pulse durations of 1 μ sec to 1 msec and beam current densities up to 50 A/cm². Detailed results are presented in Section III-B.

These results indicate that electron guns for high energy e-beam lasers can be constructed which are simpler, more efficient, and more rugged than the present guns. The new guns will simplify the construction and operation of high energy lasers. Work is continuing on expanding the beam dimensions of the plasma cathode e-gun. The high-voltage module now under construction will produce a beam 1 cm x 13 cm. Side-by-side stacking of the basic module will permit the production of very large-area beams.

I. INTRODUCTION

A. Objectives

The overall objective of this program is to develop a high voltage electron gun containing a plasma electron source and capable of being used for electron beam plasma conditioning of electric discharge lasers. This is a new type of device combining a modified low pressure hollow cathode discharge with a control grid structure to generate a well controlled high energy electron beam capable of being scaled to very large areas.

The advantages of this type of device over conventional thermionic cathodes are as follows:

Insensitivity to Contamination – Residual pressures two orders of magnitude higher than those required for thermionic cathodes can be tolerated by the plasma cathode. Thus fabrication and processing techniques can be relaxed and simplified, leading to savings of time and expense.

Improved Ruggedness – The plasma gun structure can be maintained at much lower temperature than that of thermionic cathodes. No inherently delicate heater elements are required.

Suitable for Large Area – The plasma gun can readily be scaled to large size without major difficulties (e.g., no unwieldy heater power).

Instantaneous Startup – The plasma cathode does not require heating-up time. The discharge in the plasma gun can be started within microseconds prior to the initiation of a high energy beam.

Lower Power Consumption – The plasma cathode consumes power only during the electron beam pulse, and even then the power required for the hollow cathode discharge is only a small fraction of the high energy beam power. Heater elements, which consume large

amounts of wasted power during standby periods and between pulses, are not required.

Lower Cost — The eventual cost of the plasma cathode gun should be lower than that of a comparable large area thermionic cathode because of its inherent structural simplicity and potentially greater reliability.

Several "plasma cathodes" of various types are described in the literature, and some have been used on lasers.¹ These employ one of two types of discharges: the high-voltage glow discharge or the low pressure incipient vacuum arc. The device described in this report is unlike either of these types and is expected to have the following advantages.

Better Foil Penetration for Plasma Conditioning — Better foil penetration is accomplished because the electron beam from the plasma cathode is more monoenergetic with mean energy close to the applied acceleration voltage. The other devices, in which a plasma sheath is produced in the region between the electrodes, produce a much broader energy distribution with substantial amounts of electrons at lower energy, resulting in poor foil penetration ability. There is no plasma sheath in the beam acceleration region of the present device.

Long-Pulse or CW Capability — The incipient-vacuum arc devices, which have the best foil penetration characteristics, are inherently limited to short pulse ($\sim 5 \mu\text{sec}$) operation. The device described here has produced pulses as long as 1 msec, and there appears to be no fundamental reason why it could not operate cw.

The overall objective of the program has been subdivided into several technical goals associated with the demonstration of a small scalable plasma cathode electron gun. The technical goals may be described in terms of the operational parameters of the device to be demonstrated. These parameters are as follows.

Beam dimensions	$\geq 1 \text{ cm} \times 10 \text{ cm}$
Voltage	$\geq 150 \text{ kV}$
Current density	$\geq 100 \text{ mA/cm}^2$
Pulse length	$\geq 100 \text{ } \mu\text{sec}$

The technical approach and the program organization by which these goals will be reached are the subject of Sections I-B and I-C.

B. Technical Approach

The basic concept of the plasma cathode electron gun for laser plasma conditioning is illustrated schematically in Fig. 1. A plasma source consisting of a low-pressure helium hollow cathode discharge provides electrons that are accelerated to energies of 150 kV in a plasma-free region located between the hollow cathode and the laser medium enclosure. The high energy electrons are injected into the high pressure laser medium through a thin metallic foil which separates the high and low pressure regions of the device.

To produce a high energy electron beam with a narrow energy distribution in such a gas-filled device, the number of inelastic collisions which electrons and ions make with gas molecules in the region between the accelerating electrodes must be kept to a minimum. Two reasons for this requirement are (1) every inelastic collision experienced by a high energy electron reduces its energy and decreases the mean energy of the beam, and (2) the secondary electrons produced by ionizing collisions in the acceleration region also become part of the electron beam. Since they were formed not at cathode potential but at some intermediate potential existing in the acceleration region, their energy on reaching the anode is much less than the cathode-anode voltage. These electrons therefore seriously degrade the beam energy characteristics. For the future application of the device described here to laser plasma conditioning, it is important that such beam energy degradation be eliminated because it seriously affects the beam transmission through a foil window.

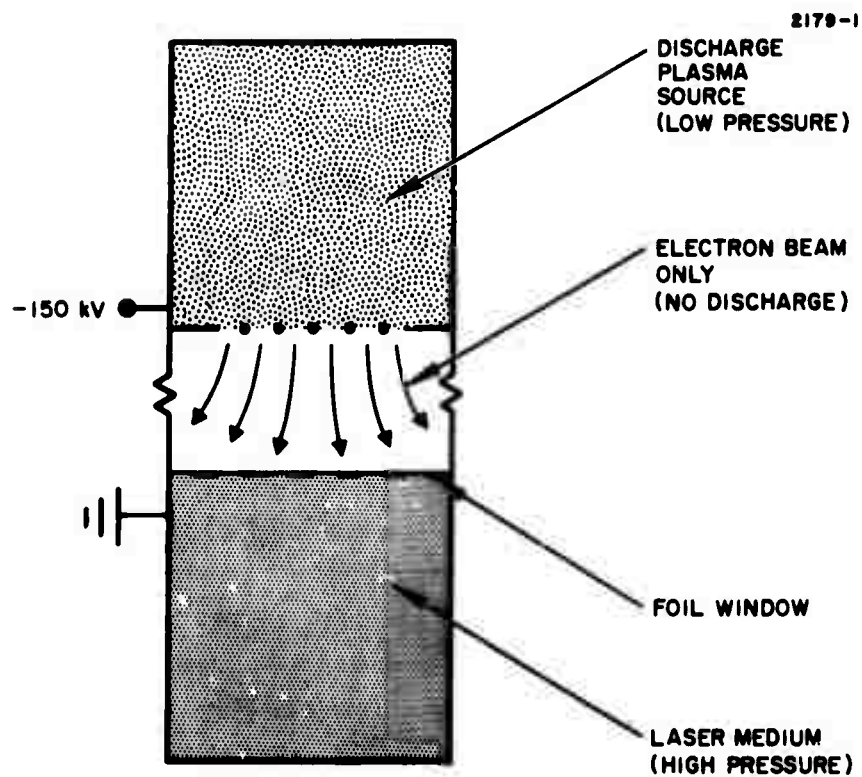


Fig. 1. Plasma cathode electron gun concept.

The minimization of inelastic collisions in the present device is achieved by operating at very low gas pressure and by separating the cathode and anode by only a short distance. This distance is determined primarily by the principles of vacuum breakdown. Previous experience has shown that properly prepared parallel-plate electrodes will conservatively withstand applied fields of approximately 70 kV/cm without breakdown in vacuum. This result is not changed if gas at very low pressures (pressures below the Paschen breakdown limit, as explained below) is added to the interelectrode region. Above 70 kV/cm field emission from microprojections on the cathode surface and other mechanisms result in breakdown into an arc discharge between the electrodes.

The lack of ionizing collisions, which are the most important inelastic collisions, may be verified by the fact that in this device there is no electrical discharge in the accelerating region. If substantial ionization were occurring in this region, avalanche breakdown would result as the secondary electrons and ions were accelerated and produced still more ion-electron pairs.

Breakdown (and inelastic collisions) are avoided by operating to the left of the Paschen breakdown curve. Paschen breakdown data for helium obtained earlier at HRL are shown in Fig. 2. The curve shows the applied voltage at which electrical discharge breakdown will occur in helium for specified experimental conditions. It can be shown that this voltage is only a function of the product $p \times d$, where p is the helium pressure expressed at standard temperature and d is the spacing between parallel-plate electrodes. In the case of nonparallel electrodes d may be considered approximately as the distance between any two points on the electrodes, so that a given set of nonparallel electrodes is characterized by a range of values of d bounded by the minimum and maximum values of electrode separation. Consideration of the curve of Fig. 2 to the left of the minimum, which is the region of interest for this device, shows that as the applied

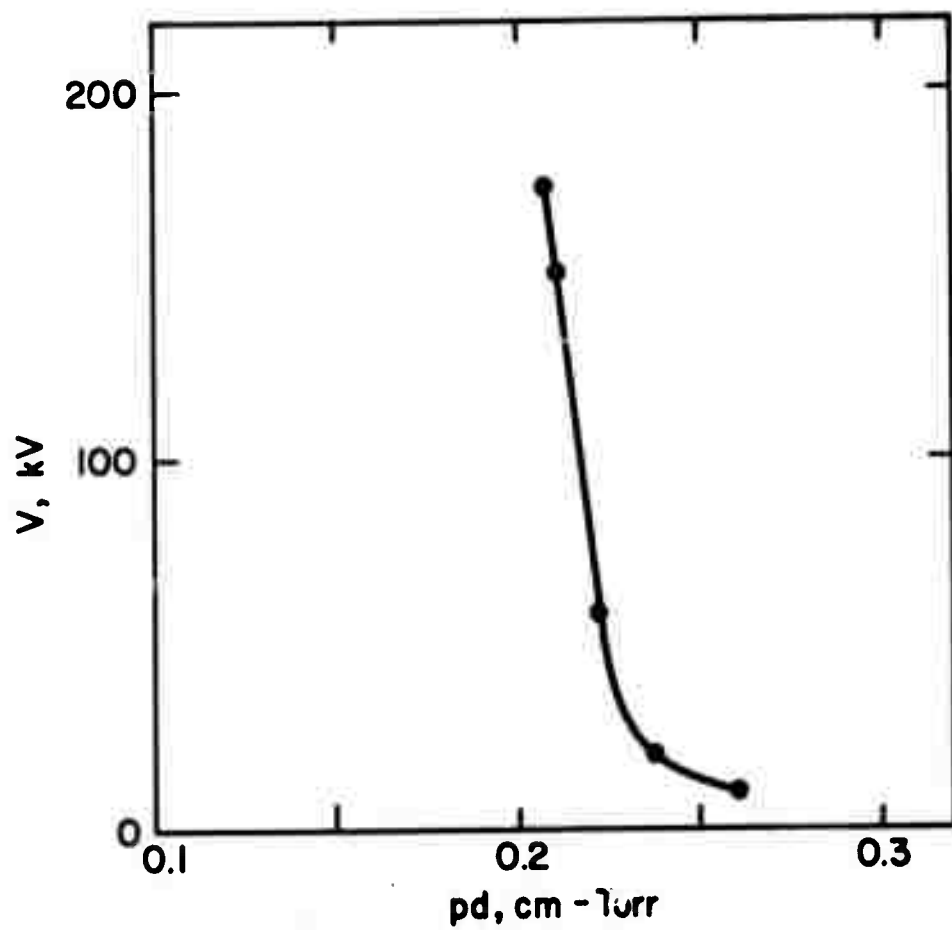


Fig. 2. Paschen breakdown in helium.

voltage is increased for a given electrode configuration and pressure, the eventual breakdown voltage is determined by the point of maximum separation of the electrodes.

The Paschen breakdown voltage decreases as electrode spacing is increased. This is the opposite behavior from vacuum breakdown, in which the breakdown voltage decreases as the electrode separation decreases. The allowable electrode separation for a given operating voltage and pressure therefore has a lower limit, determined by vacuum breakdown, and an upper limit, determined by Paschen breakdown. If the electrode spacing is nonuniform, both the most closely and most widely separated points must lie within the bounds set by the two types of breakdown. This behavior is illustrated in Fig. 3 where the vacuum breakdown and Paschen breakdown voltages are shown as a function of electrode separation at an operating pressure of 50 mTorr of helium. All the plasma cathode devices investigated in this program are designed to operate without either type of breakdown in the beam acceleration region.

Of course, at the same time, it is necessary to produce a plasma in the plasma generation section of the gun as the source of the beam electrons. Since the constraints of vacuum breakdown and Paschen breakdown require operation of the device at low pressures if high beam voltages are to be attained, a special type of discharge is necessary in the plasma generation section. This discharge must ignite quickly and reliably, operate stably, and produce sufficient plasma density to furnish electrons for the beam, all at rather low gas pressures. Two types of discharge that fulfill these requirements are the crossed-field discharge and the hollow cathode discharge. Both these types have been investigated experimentally as part of the current program. The theory of these discharge types and the experimental results obtained are described in Section II. The theoretical and experimental details of the interface region between the plasma generation and beam acceleration sections, called the electron extraction section, are presented in Section III.

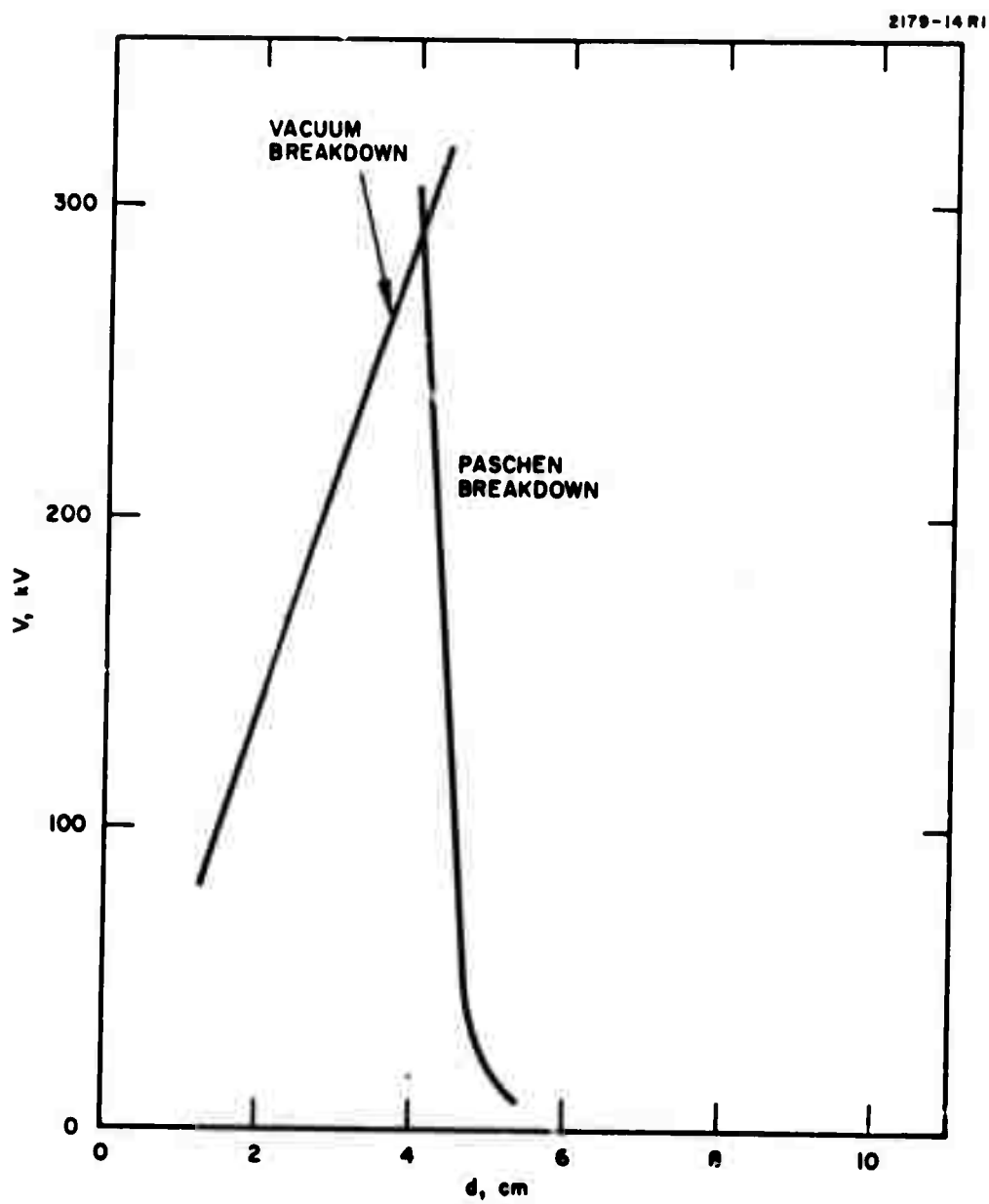


Fig. 3. Low pressure breakdown characteristics.

C. Program Organization

To accomplish the technical objectives of this contract, the program has been divided into four principal tasks: Discharge Studies, Low-Voltage Electron Extraction, Paschen Breakdown Experiments in the Presence of an Electron Beam, and High Voltage Rectangular Gun including Beam Diagnostics.

Task 1: Discharge Studies

The goal of this task is to develop a discharge configuration that will produce the plasma density required for extracting a 150 kV electron beam with $\geq 100 \text{ mA/cm}^2$. The discharge device must be capable of operating at very low pressures in order to avoid Paschen breakdown problems in the beam acceleration region as explained previously. As part of this task, crossed-field, hollow cathode, and hybrid configurations were investigated experimentally. These experiments, together with experiments on plasma ignition methods, were done in a small scale cylindrical device of diameter 3.6 cm and length 5 cm. The configuration which performed best for the intended use was then built in a full size rectangular version for the high voltage gun of Task 4.

Task 2: Low-Voltage Electron Extraction

This task was directed toward developing and testing an electron extractor. The extractor is located between the plasma generation section of the gun and the beam acceleration region (see Fig. 4). The extractor extracts electrons from the plasma in a beam and passes them to the accelerator section. It also shields the plasma section and accelerator section from each other, allowing breakdown in the former, but not the latter, and preventing the high electric field of the accelerator from perturbing the plasma region. The initial experiments were performed with a small, low-voltage extractor and accelerator built to operate with the small-scale device of Task 1. From the results of the experiments the extractor for the full-size device of Task 4 was designed and built.

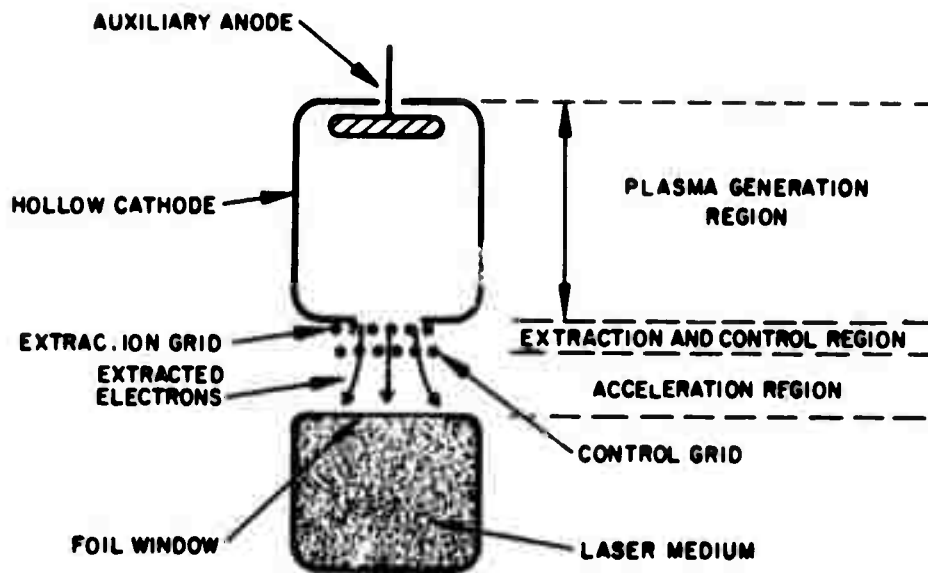


Fig. 4. Plasma cathode electron gun schematic.

Task 3: Paschen Breakdown in the Presence of an Electron Beam

Gas breakdown properties in helium at low pressures have been measured by many investigators.³⁻⁵ There is, however, considerable disagreement among the published results. In addition, the effect of a high-energy electron beam on the breakdown properties has not been investigated previously. For these reasons, an experimental device was designed and built which measures the breakdown voltage both with and without the electron beam. The electrode configuration employed in the device resembled the high voltage device of Task 4, but the electron beam was of smaller area and was provided by a thermionic cathode. The device and experimental results are described in Section IV.

Task 4: High Voltage Device and Beam Diagnostics

The design, fabrication, and testing of a high voltage rectangular (1 cm x 13 cm) plasma cathode electron gun constitute the effort of this task. The design of the device is described in Section V. No experimental work has been performed yet on this task during this reporting period. The experimental results, operating characteristics, and beam parameters of the device will be described in the final Technical Report.

II. LOW PRESSURE DISCHARGE CONFIGURATIONS

A. General

1. Types of Discharges Investigated

The initial experimental effort in this program was directed toward finding a suitable discharge plasma source for the plasma cathode e-gun. The requirements for the plasma source include reliable ignition operation at moderate voltage, and the ability to produce reasonably dense plasmas at very low gas pressure. The requirement for low gas pressure arises from the need to avoid Paschen breakdown in the high voltage section of the gun.

Among the types of discharge which were believed likely to fulfill the necessary requirements were the crossed-field and the hollow cathode discharges. The present studies were begun with a crossed-field discharge as the plasma source for the plasma cathode e-gun in order to compare with earlier experience at HRL with this discharge type. This type of discharge ignites easily and will produce large plasma densities at very low gas pressure. A cylindrical configuration with radial electric field and longitudinal magnetic field was employed, as shown in Fig. 5. The results of this investigation were similar to those obtained earlier by other investigators at HRL.

Because of the way in which the anode intrudes into the cathode structure of the crossed-field discharge, extraction of electrons from the discharge plasma would be geometrically difficult. For this reason a modified version of the familiar hollow cathode discharge was next investigated. The intruding anode of the previous crossed-field device was replaced with a button anode of the same diameter which effectively formed one end of the cylindrical structure. The cathode was placed as before in a longitudinal magnetic field. After ignition the characteristics of this type of hybrid discharge should be similar to the crossed-field discharge tested first, at least at high cathode current density, because the electric and magnetic field configuration will be similar.

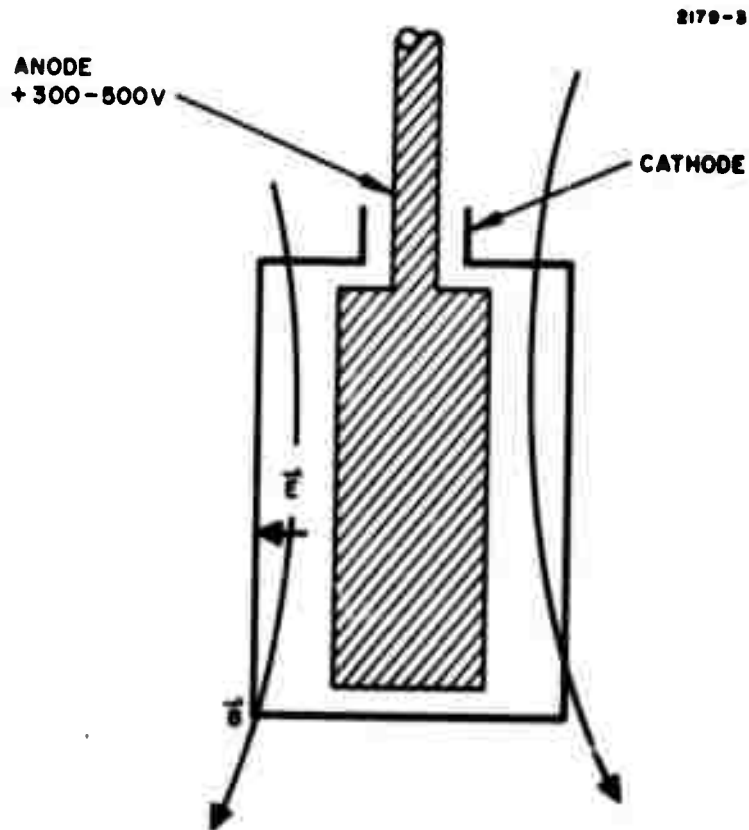


Fig. 5. Crossed-field discharge device.

A sheath will be formed parallel to the cathode surface with thickness much less than the cathode diameter. Much of the discharge voltage will appear across the sheath, so the electric field will be perpendicular to the cathode (and to the magnetic field) as before.

The ignition characteristics of this type of discharge were not known previously. They proved to be inconvenient for the present application, since rather large ignition voltages were required. In addition, the magnetic field requirement necessitated a bulky solenoid. In the interest of simplification a third discharge configuration will be tested. It may have all the necessary characteristics and require no magnetic field. It consists of the hollow cathode cylinder with a very thin (0.010 in.) on-axis wire anode, as shown in Fig. 6. A detailed discussion of results obtained with this configuration will be presented in the Final Technical Report.

2. Experimental Device

The experimental device with which the previously mentioned studies were conducted was designed as a versatile test vehicle which could be easily modified to produce different discharge configurations. After additional modifications the device was used for preliminary electron extraction experiments. An external view of the experimental tube is shown in Fig. 7. Although the external appearance of the tube changed very little, major changes were made to the interior anode structures to provide the various types of discharges investigated. The common cathode used in all these experiments is shown in Fig. 8 with the crossed-field anode. When the long anode was used the electric field was radial and the device produced a crossed-field discharge. When a short button anode was used the device operated as a hollow cathode discharge tube.

The avoidance of spurious discharges between the electrodes in regions other than the desired discharge region must be given careful attention in low pressure discharge devices of this type. The mechanisms causing such discharges (vacuum breakdown and Paschen breakdown) are well understood and their effect must be included quantitatively

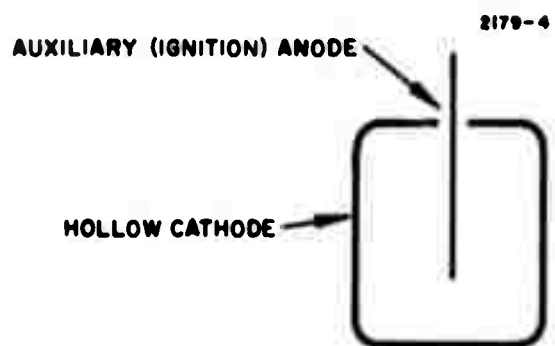


Fig. 6. Hollow cathode discharge ignition test vehicle.

M8915

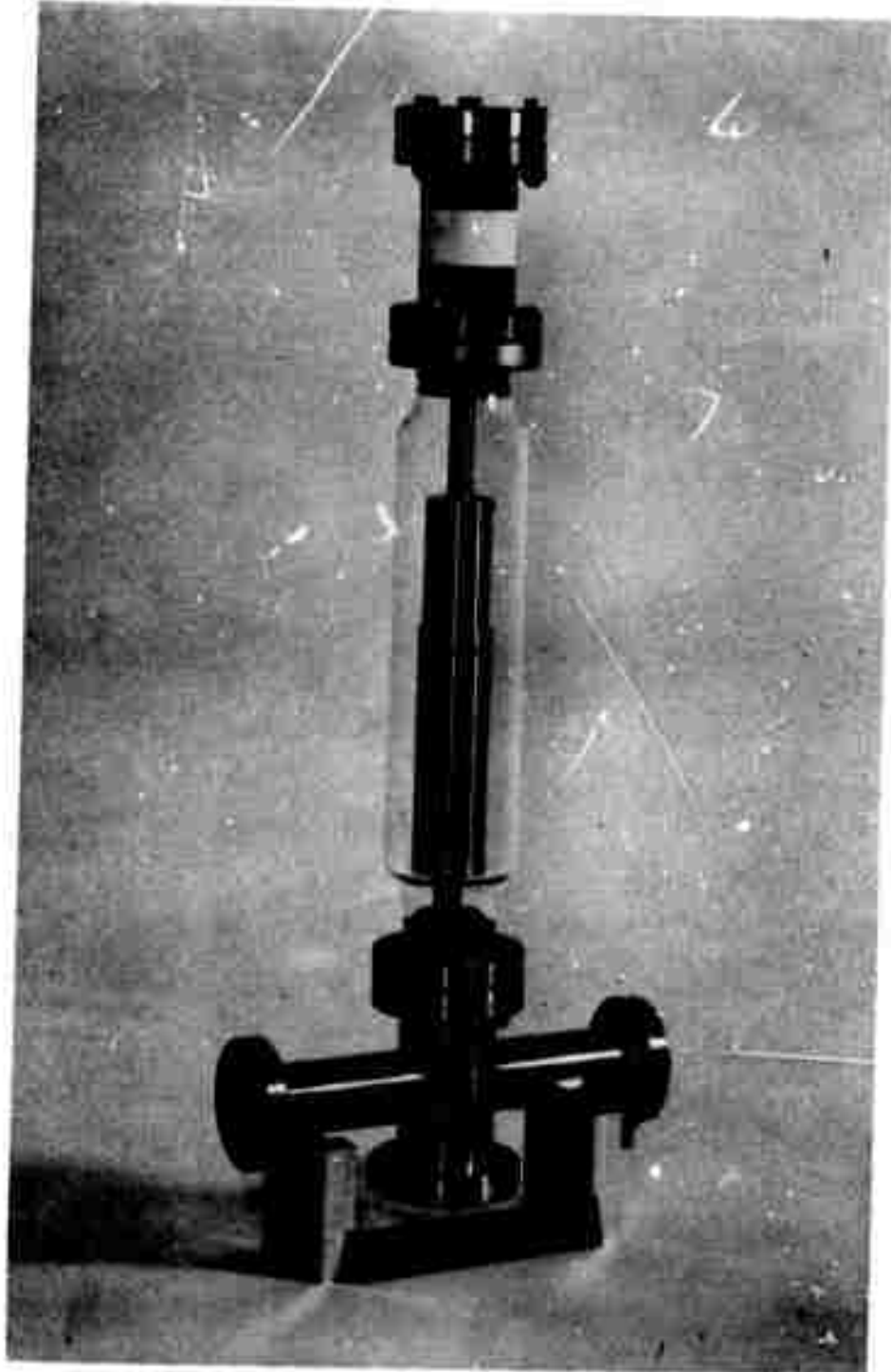


Fig. 7. Low voltage plasma cathode E-gun device.

M8914

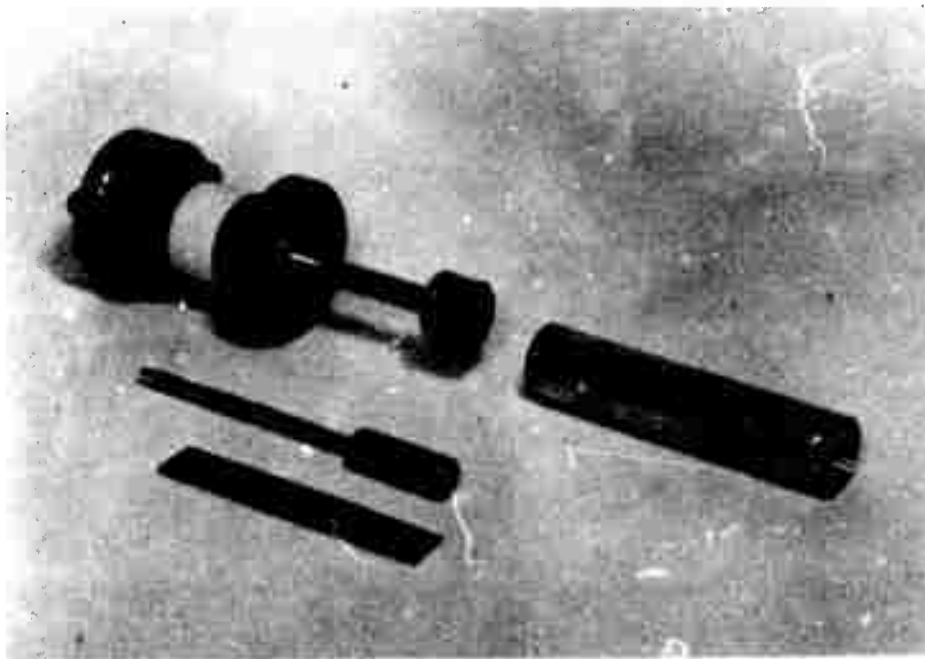


Fig. 8. Cathode and crossed-field tube anode.

in the design. Because the problems encountered in the design of the electrode feedthroughs of the present tube are characteristic of those encountered in low-pressure discharge devices in general, including the final plasma cathode electron gun, the design of these feedthroughs, which is shown in Fig. 9, will be briefly described here.

At these low gas pressures (≤ 50 mTorr) of helium), the mean free path for ionization by electron impact is long compared with the characteristic dimensions of the discharge tube. Therefore, the usual type of gas discharge breakdown (Paschen breakdown), which develops as an avalanche process of electron impact ionizations in an applied electric field, occurs between the most widely separated electrode surfaces, rather than between the most closely spaced surfaces.

At very high applied electric fields, however, vacuum breakdown⁷ occurs between the most closely spaced surfaces and results in a discharge. Its occurrence is practically independent of gas pressure, at least at low pressures. It is strictly dependent on the electric field at the electrode surfaces. To prevent this type of breakdown, all electrode surfaces must be polished carefully to remove sharp edges, points, and protrusions. Adequate clearance between the electrode surfaces must be allowed at all places inside the tube.

Therefore, the discharge tube design must take account of the vacuum breakdown process occurring between the most closely-spaced areas of the electrodes and Paschen breakdown process occurring between the most widely separated areas.

To apply these concepts to the present tube it is necessary to choose an operating pressure and an operating voltage for the design, as well as to determine the Paschen breakdown parameter, which is a product of (gas pressure) x (electrode spacing). A conservative value for the Paschen breakdown parameter in helium under the conditions for which this tube was designed is 0.2 cm-Torr. The drawing of the electrode feedthrough structure in Fig. 9 shows that the minimum separation between the anode and cathode connections in the feedthrough regions (at A, for example) is 0.3 cm. The maximum separation (at B)

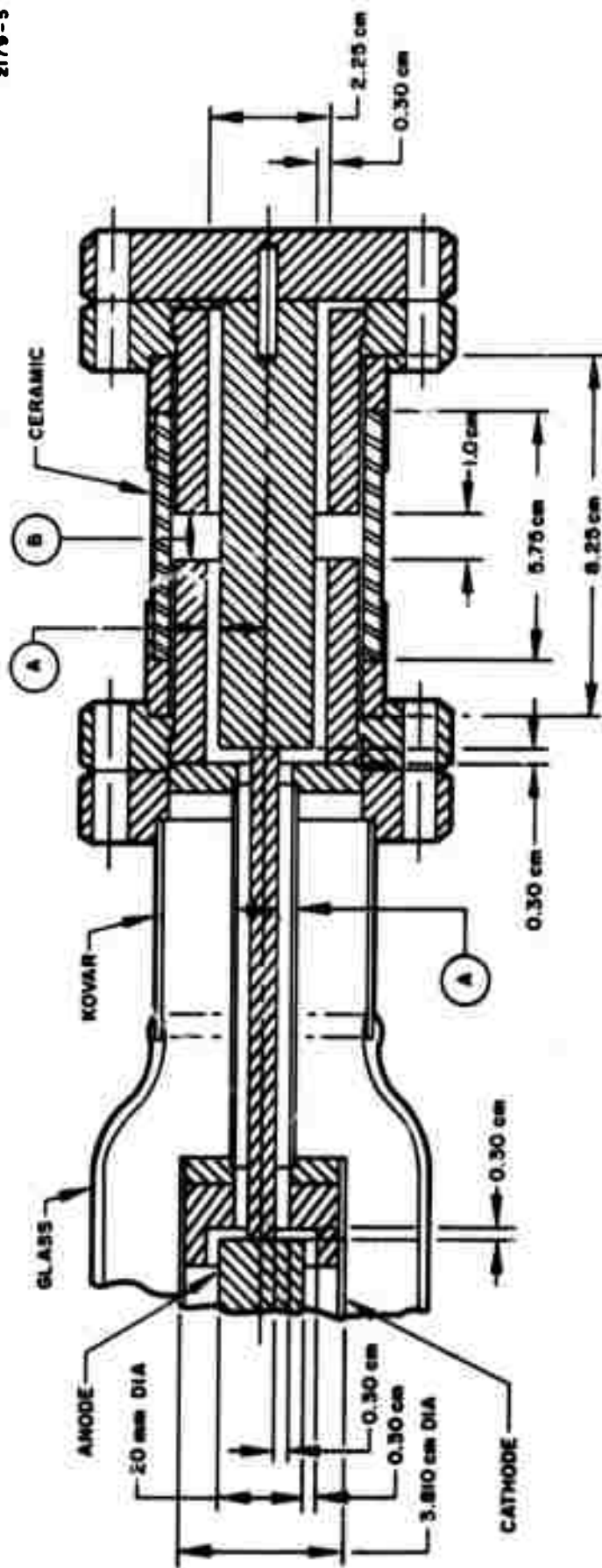


Fig. 9. Anode feedthrough design of experimental tube.

is 1.0 cm. All sharp edges have been rounded and all the metal parts have been electropolished and acid-treated to remove any sharp surface irregularities. With these dimensions and the data of Fig. 2, it is clear that no Paschen breakdown will occur in the feedthrough region provided the helium pressure is maintained below 200 mTorr, for at this pressure $p \times d$ the product of (gas pressure) \times (electrode spacing), reaches the Paschen breakdown value of 0.2 cm-Torr in the region where the electrode separation is 1.0 cm. In addition, vacuum breakdown will occur in the feedthrough region when the applied voltage exceeds about 23 kV. At this time, the applied field will be 70 kV/cm in those regions where the electrode spacing is 0.3 cm. The value of 70 kV/cm is achievable in technical applications with reasonable care in surface preparation of the electrodes.

The fact that the field at the surface of the anode feedthrough cylinder is somewhat higher than 70 kV/cm under these conditions because of the cylindrical geometry is not important; since vacuum breakdown is apparently initiated by field emission from the negative electrode surface for gaps of this size and stainless steel electrodes, it is the field at the cathode surface that is most important.

In summary, the well-known principles of vacuum and Paschen breakdown are very important in the design of structures like that of Fig. 9 and will be used many times in this program. For this feedthrough structure, these principles predict the maximum operating pressure, 200 mTorr, and the maximum operating voltage, 23 kV.

E. Crossed-Field Discharge

1. Theory

The basic mechanism of the crossed field discharge is simple. The electrode and field configurations are as shown in Fig. 5 in the present experiments. The spacing between electrodes is smaller than the mean free path for ionization. In the absence of the magnetic field there can be no breakdown because the usual avalanche ionization

process by which the glow discharge develops cannot occur. The addition of the magnetic field, however, causes the electrons to move in cycloidal paths, increasing the effective path length so that ionizing collisions occur and the ionization avalanche breakdown takes place. The magnetic field affects the trajectories of the ions very little because of their much larger mass. After each inelastic collision the kinetic energy of the electron is greatly decreased and it begins to trace a new cycloidal path which is again interrupted by collisions. The resulting electron trajectory is shown schematically in Fig. 10. If the applied voltage is too high or the magnetic field is too small the cycloidal path of the electrons intercepts the anode and the device no longer operates as a crossed-field unit, so the discharge will not ignite. The upper voltage limit V_B is given by

$$V_B < \frac{B^2 \times d^2}{11.36}$$

B in gauss
d in cm
 V_B in volts

Previous experiments with this type of discharge⁶ have shown that the ion energy distribution at the cathode is monoenergetic with its peak approximately equal to the discharge voltage. This fact suggests that the potential in the main body of the plasma, where the ions are formed, is close to the anode potential. The cathode fall is thus approximately equal to the discharge voltage. The thickness of the cathode sheath may be calculated as follows. The discharge current is composed of ions arriving at the cathode plus electrons leaving the cathode. The ratio of electron current to ion current is γ , the secondary emission coefficient for the particular ion, ion energy, and cathode material. For the present case $\gamma \approx 0.15$. The ion current J_+ may be related to the sheath thickness l_s and the voltage drop across the sheath V_s by the Child-Langmuir space-charge equation^{8,9}

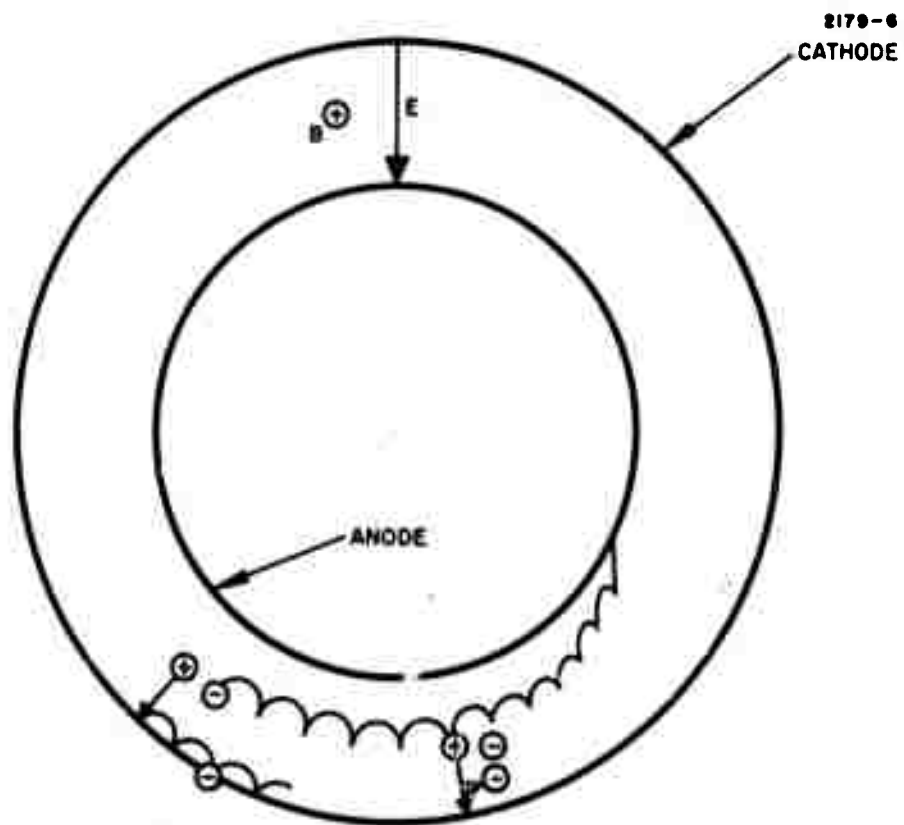


Fig. 10. Electron and ion paths in a coaxial cylindrical crossed-field geometry.

$$J_+ = \left(\frac{2e}{M}\right)^{1/2} \frac{4\epsilon_0}{9} \frac{V_s^{3/2}}{l_s^2} \quad (1)$$

where e and M are the ion charge and mass and ϵ_0 is the permittivity of free space. In addition,

$$J = J_+ + J_- = J_+(1 + \gamma) \quad (2)$$

Combining eqs. (1) and (2) and solving for l_s yields

$$l_s = \left[\frac{(1 + \gamma)}{J} \left(\frac{2e}{M}\right)^{1/2} \frac{4\epsilon_0}{9} V_s^{3/2} \right]^{1/2} \quad (3)$$

Typical parameters are

Discharge current	= 1 A
Cathode area	= 55 cm ²
∴ Cathode current density = J	= 18 mA/cm ²
γ	= 0.15
V_s	= 300 V

The calculated value of the sheath thickness for these operating conditions is approximately 0.1 cm. The resulting potential distribution in the tube is shown qualitatively in Fig. 11.

These results may be used to predict theoretically the discharge operating voltage as follows. The cathode current is determined by ion diffusion out of the main plasma volume. The ions are accelerated across the cathode sheath and strike the cathode, yielding secondary electrons which are accelerated across the sheath in the opposite direction, back into the main plasma volume. Here they produce ions by colliding with neutrals, but since the potential in the volume is almost

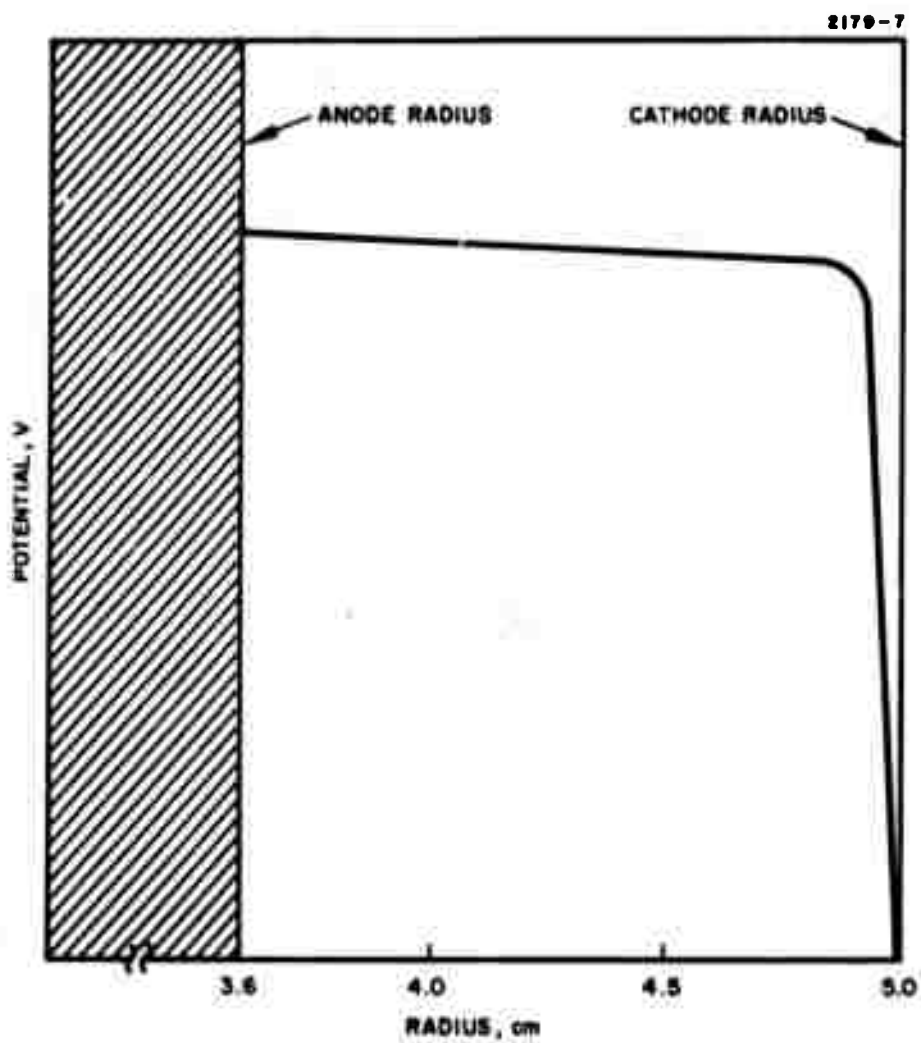


Fig. 11. Qualitative potential distribution in crossed-field tube.

uniform (Fig. 11) they gain no additional energy. Each ion diffusing out of the plasma and striking the cathode produces γ electrons, where γ is the secondary emission yield and is typically 0.15 for helium ions and stainless steel cathodes. Conservation of the total ion density then requires that each electron accelerated through the sheath must produce γ^{-1} ions. The sheath potential (cathode fall) V_C must then be at least

$$V_C \geq \gamma^{-1} \times V_i$$

where V_i is the ionization potential of helium, 24.6 V. Thus $V_C \geq (24.6/0.15) = 164$ V. The discharge voltage may be larger than this value as a result of other inelastic collision and loss processes in the device. The experimentally observed value of the discharge voltage was approximately 300 V, with little dependence on current (as expected).

The minimum operating pressure of the crossed-field discharge is rather difficult to predict quantitatively. To obtain the type of discharge represented by the potential of Fig. 11, the ions must cross the electrode gap more slowly than the electrons. If the electrons cross the discharge more slowly, most of the voltage drop would appear at the anode.

Decreasing the pressure decreases the transit time across the discharge for the ions because it decreases the number of ion-neutral collisions and allows the ions to move more directly along the electric field lines, which represent the shortest distance from cathode to anode. Because of their large mass the ions are affected very little by the magnetic field.

Decreasing the pressure increases the electron transit time across the discharge, however, because it decreases the number of collisions and forces the electrons to move in longer trajectories. This effect is illustrated in Fig. 10. The electron orbit caused by the crossed electric and magnetic fields is smaller in diameter than the electrode spacing. Therefore, in the absence of collisions the electrons

would not cross the discharge at all. Only the effect of collisions in interrupting the circular orbits allows the electrons to cross the discharge. The higher the pressure, the more collisions, and the shorter the electron transit time becomes.

The critical pressure P_c can be calculated by setting the ion and electron transit times equal. To calculate the transit times requires knowledge of the electric field in the main discharge region, however, as well as accurate values for electron and ion mean energies. Since these quantities are unknown in the present experiments, no estimation of P_c is possible without considerable additional experimental effort. A much simpler approach is to use the theory just described to predict the qualitative effect of various parameters on P_c and to obtain the actual value of P_c by direct measurement.

2. Experimental Results

The motivation for studying experimentally this type of discharge was merely to obtain a standard for comparison with the hollow cathode discharge. It was believed that the two discharges should exhibit similar characteristics in the steady state, because, as explained in Section II-A, the presence of the cathode sheath and resulting cathode fall in the hollow cathode discharge constrains the effective electric field to be radial, at least after the plasma ignites and the sheath forms. Since the magnetic field is longitudinal, and perpendicular, the discharge becomes a "crossed-field hollow cathode discharge."

The data obtained for the true crossed-field discharge consisted of voltage-current characteristics of the discharge for different values of helium pressure and magnetic field. The theoretical expectation, as discussed earlier, combined with the experimental results of earlier workers, indicated that the discharge voltage should be nearly independent of current over a wide range of current for constant pressure and magnetic field. In addition, it was expected that the discharge voltage should fall with increasing gas pressure at constant current and magnetic field and that the voltage should be roughly independent of magnetic

field above a certain critical value of the magnetic field. The critical value of magnetic field was expected to be inversely related to the operating pressure.

All of the theoretical expectations were fulfilled by the experimental data obtained. To obtain the data the tube was pulsed with a Velonex pulser while the current was read from the voltage drop across a calibrated resistor and the voltage was measured with a high voltage probe. Both quantities were displayed on an oscilloscope. The pulse length in all the measurements was 200 μ sec, and the repetition frequency was less than 10 Hz. Helium pressure was measured using a calibrated Hastings-Raydist thermocouple gauge with a correction chart for helium supplied by the manufacturer.

Some of the data obtained is shown in Figs. 12 through 16. Each figure shows the behavior of discharge voltage with discharge current, with magnetic field as a parameter, for a different operating pressure. The curves display clearly the independence of voltage from current and magnetic field. The discharge voltage decreases slightly with increasing gas pressure when the discharge current and magnetic field are held constant, as shown in Fig. 17. The critical minimum operating magnetic field decreases with increasing pressure.

This crossed-field discharge ignited at an applied voltage which was almost independent of magnetic field, provided that the field was strong enough to permit crossed-field operation. The ignition voltage was only slightly higher than the operating voltage. These features agree well with detailed observations by others.

These results verified that the experimental design was sound and that the necessary auxiliary equipment operated as intended. The results also provided a data base for the investigation of the hollow cathode discharge. The conversion of the experimental tube to a hollow cathode type was carried out as described previously merely by replacing the protruding anode with a flat one (Fig. 8).

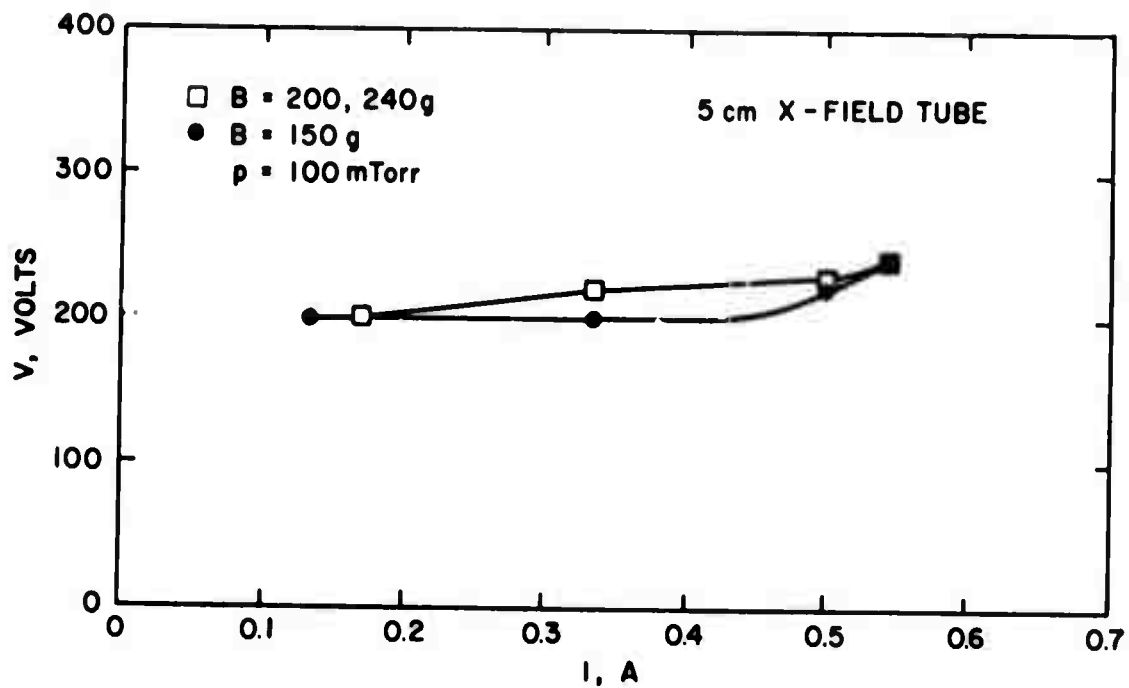


Fig. 12. Crossed-field tube voltage-current characteristics, $p = 100$ mTorr.

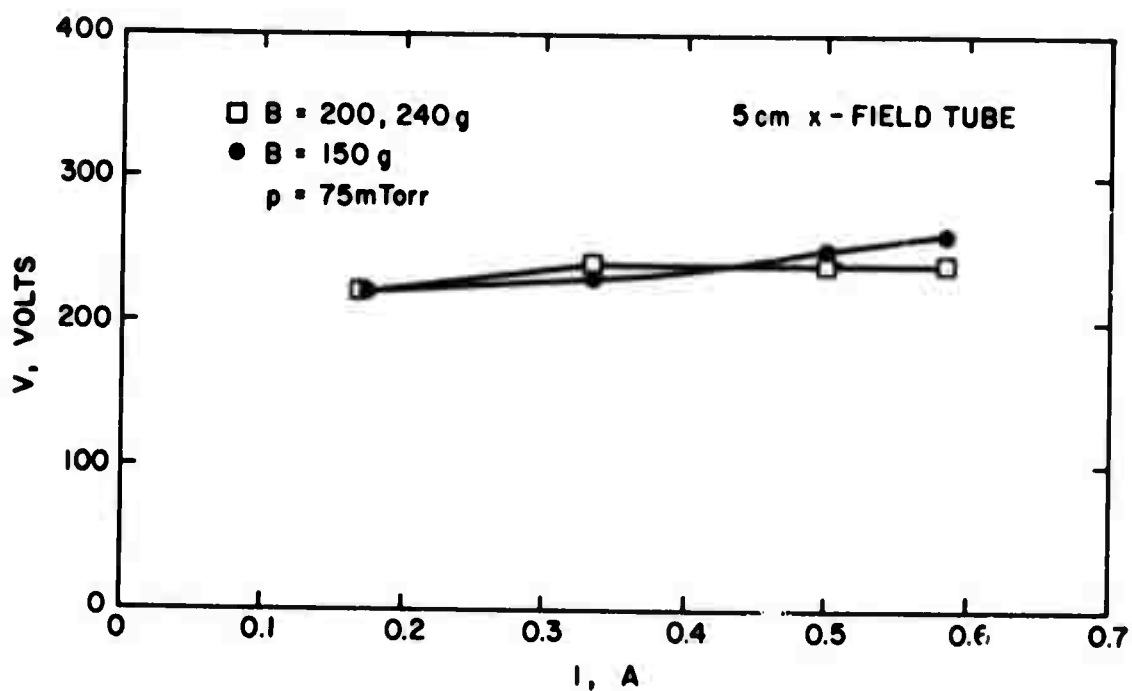


Fig. 13. Crossed-field tube voltage-current characteristics, $p = 75$ mTorr.

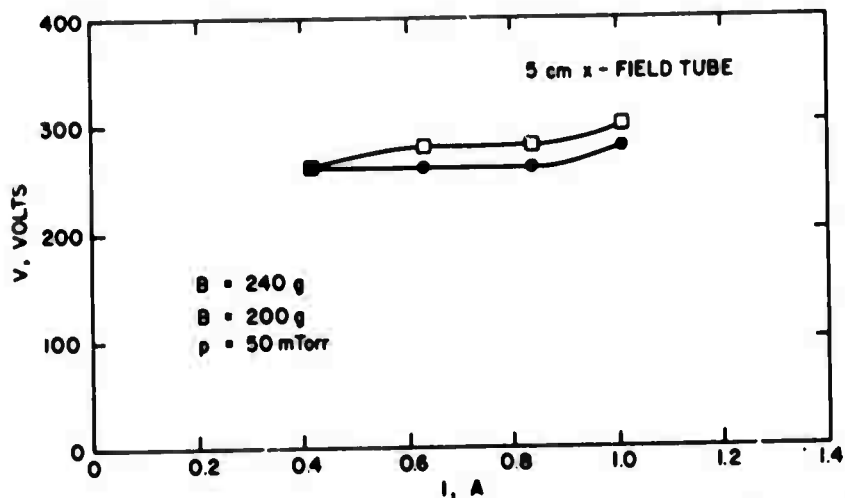


Fig. 14. Crossed-field tube voltage-current characteristics, $p = 50 \text{ mTorr}$.

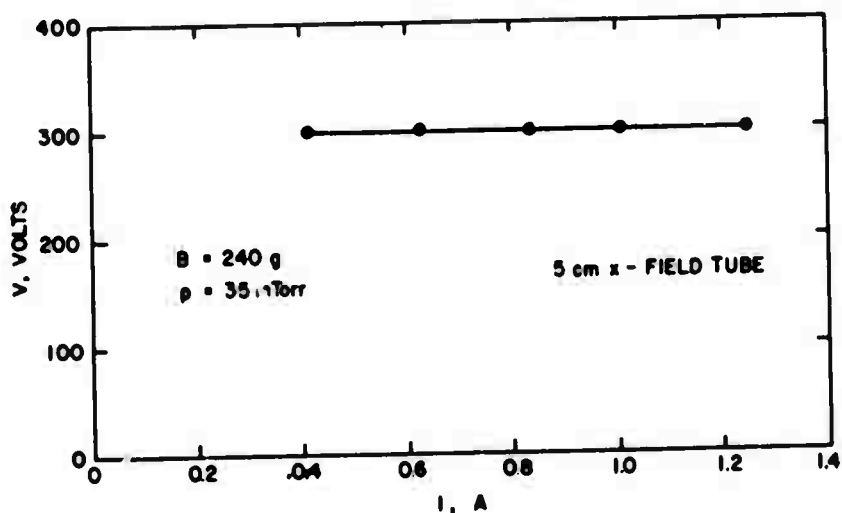


Fig. 15. Crossed-field tube voltage-current characteristics, $p = 35 \text{ mTorr}$.

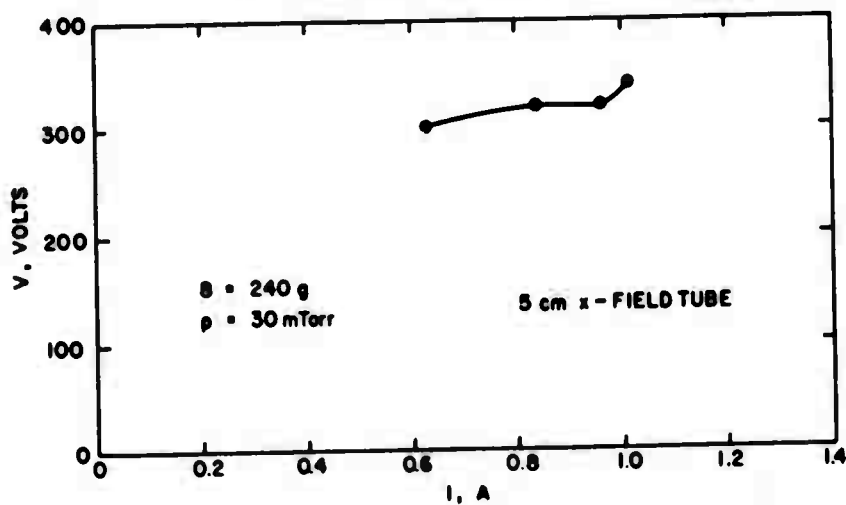


Fig. 16. Crossed-field tube voltage-current characteristics, $p = 30 \text{ mTorr}$.

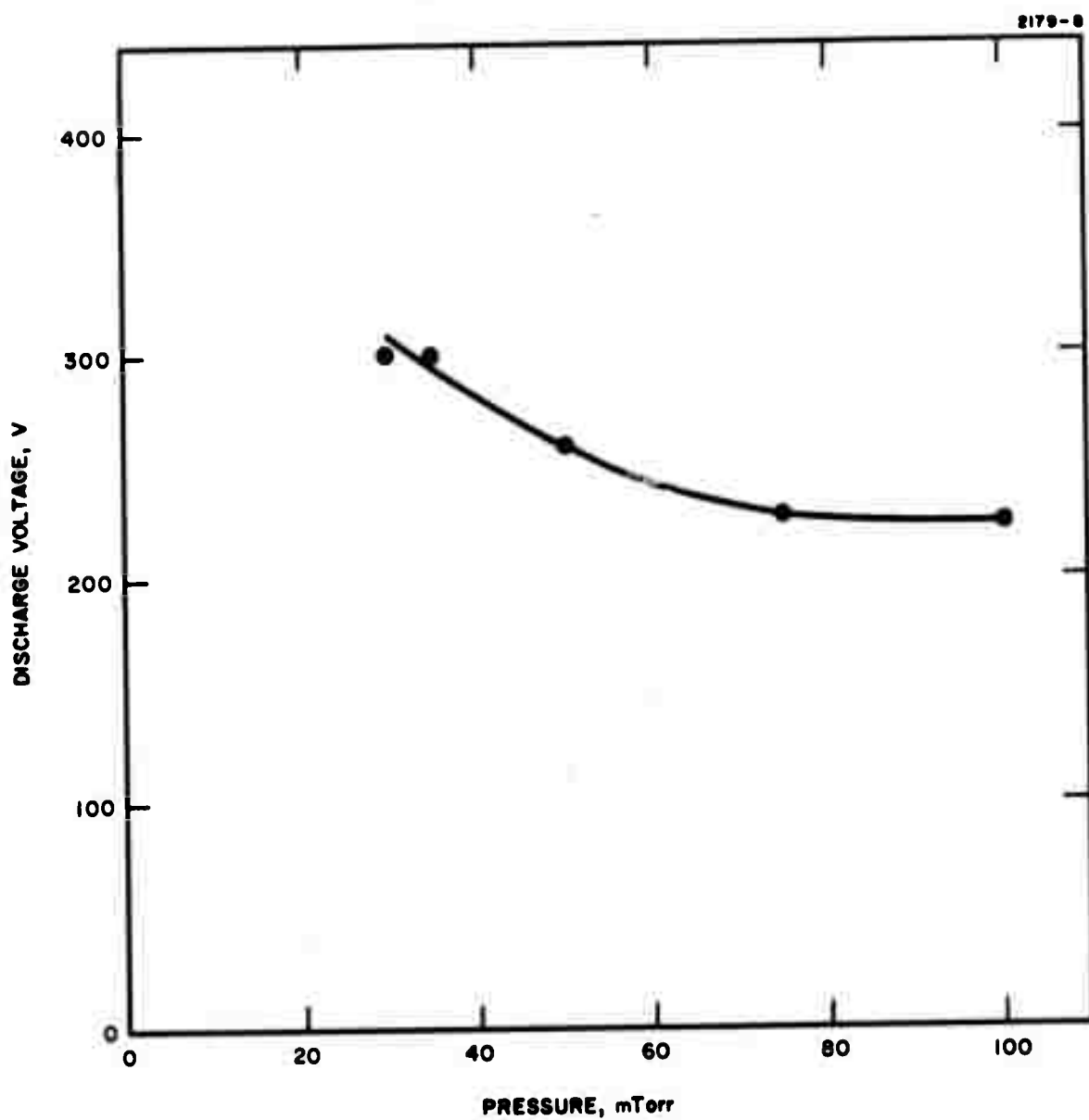


Fig. 17. Crossed-field tube voltage as a function of gas pressure with $B = 240$ g and $I = 0.6$ A.

C. Hollow Cathode Discharge

1. Theory

The hollow cathode discharge configuration considered is that illustrated in Fig. 18. The major purpose of this theory is to determine if the minimum pressure at which such a hollow cathode discharge can be sustained in the desired mode without a magnetic field is as low as required by the Paschen breakdown constraints of the present device. Elimination of the magnetic field would simplify the device and make adaptation to rectangular geometry much simpler.

The principal predictions of the theory presented here are the approximate minimum operating pressure of the hollow cathode discharge and the approximate discharge voltage. As in the crossed-field discharge, in this type of discharge at these pressures the plasma potential is close to the anode potential. Most of the discharge voltage appears across the cathode sheath, which is of the "free fall" (collisionless) type. Ions from the plasma are accelerated through the cathode sheath to the cathode surface, which they strike, producing secondary electrons, which are themselves accelerated through the sheath in the reverse direction, back into the plasma. For each ion incident on the cathode surface γ secondary electrons are produced. γ is called the secondary emission coefficient and is a function of the type of ion, the ion energy, and the type of cathode surface. For the present conditions, we estimate $\gamma \approx 0.15$.

The approximate discharge voltage may be calculated using the same method used in the crossed-field discharge. In steady-state the number of ions leaving the plasma must equal the number generated in the plasma. The principal ion generation mechanism in the plasma is electron impact ionization of neutral gas molecules. Since each ion produces γ electrons at the cathode surface, each electron must produce $N = 1/\gamma$ ions in the plasma after acceleration through the sheath. Therefore, the electron energy after acceleration through the sheath, eV_s , must be at least NE_i , where E_i is the ionization energy of helium, i. e.,

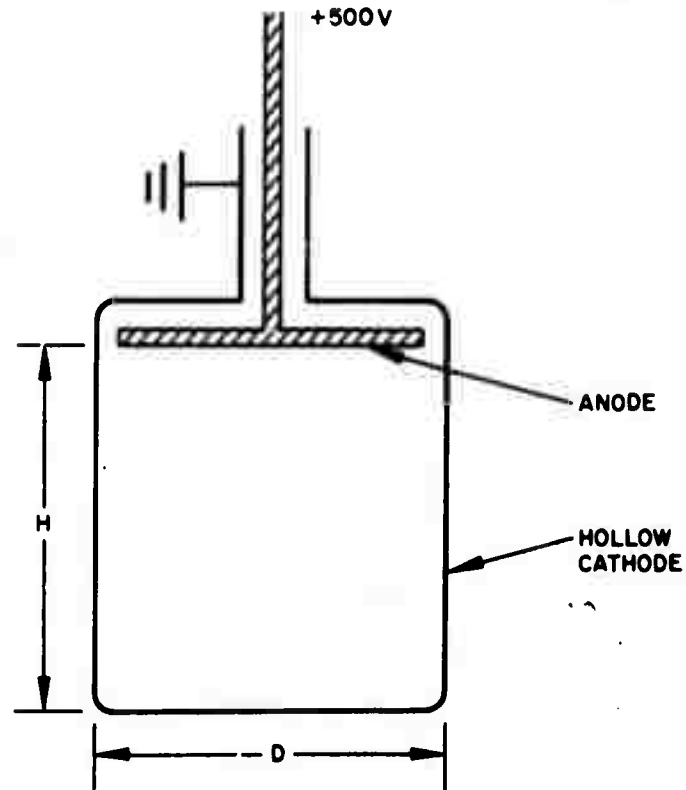


Fig. 18. Hollow cathode discharge configuration.

$$eV_s \geq NE_i$$

The discharge voltage V_D is approximately equal to V_s , the potential difference across the cathode sheath.

$$V_D \approx V_s$$

$$E_i = 24.6 \text{ eV}$$

$$N = \frac{1}{\gamma} = \frac{1}{0.15} = 6.7$$

Therefore,

$$V_D \geq 6.7 \times 24.6 = 164 \text{ volts}$$

This approximate result is independent of pressure, current, and electrode structure of the discharge. The observed range of all discharge voltages in the present experiments exceeded this predicted minimum value. The observed minimum discharge voltage was about twice as large as the predicted minimum voltage, which is a reasonable agreement considering the approximate nature of the theory.

If the electrode configuration of the discharge is specified, the minimum operating gas pressure can be theoretically predicted. Let the cathode area be A_i and the anode area A_a . As shown above in the prediction of minimum discharge voltage, each electron leaving the cathode must produce N ions, where $N = 1/\gamma$. Therefore the total path length l of the electron in the plasma from the time it is emitted at the cathode until it reaches the anode must satisfy the inequality

$$l \geq N\bar{\lambda}_i \quad (4)$$

where $\bar{\lambda}_i$ is a suitably averaged value of the mean free path for electron impact ionization. The mean free path λ_i must be averaged because it is a function of the incident electron energy. It may be expressed as

$$\lambda_i(E) = \frac{2.8 \times 10^{-17}}{p\sigma_i(E)} \text{ cm} \quad (5)$$

where p is the gas pressure in Torr at 0°C and $\sigma_i(E)$ is the ionization cross section as a function of electron energy. Combining eqs. (4) and (5) yields

$$l > \frac{N}{p\bar{\sigma}_i} \times 2.8 \times 10^{-17} \text{ cm} \quad (6)$$

To determine l it is assumed that an electron emitted from the cathode surface traverses the plasma and is reflected by the sheath of the opposite wall. It is additionally assumed that the direction of electron motion is randomized before the electron reaches the anode. After each collision with the sheath the probability that the electron will be captured at the anode before making another collision with the cathode is then approximately A_A/A_C , the ratio of anode-to-cathode area. Therefore, on the average, an electron will make C collisions with the cathode sheath before hitting the anode, where

$$C = A_C/A_A$$

The average distance L traveled by an electron between collisions with the cathode sheath may be calculated from the electrode geometry. The total distance l traveled by the electron before escaping to the anode is

$$l = CL = \frac{A_C L}{A_A} \quad (7)$$

Combining eqs. (6) and (7) and inverting,

$$\frac{p\bar{\sigma}_i}{N \times 2.8 \times 10^{-17}} \geq \frac{A_A}{A_C L}$$

$$p \geq \frac{A_A \times N \times 2.8 \times 10^{-17}}{A_C \times L \times \bar{\sigma}_i} \text{ Torr} \quad (8)$$

which gives the minimum pressure p_{\min} for operation of the hollow cathode discharge.

For the cylindrical device used in these experiments p_{\min} can be calculated from eq. (8) as follows. For a right circular cylinder of approximately equal diameter D and height H , the distance L may be approximated by

$$L = \left[\left(\frac{2D}{\pi} \right)^2 + \left(\frac{H}{2} \right)^2 \right]^{1/2}$$

In the present case $D = 3.6$ cm, $H = 5.0$ cm, therefore $L = 3.4$ cm. In addition,

$$A_C \approx \pi DH + 2 \left(\frac{\pi D^2}{2} \right) - A_A = 96.4 \text{ cm}^2$$

$$A_A = \pi(.5)^2 = 0.785 \text{ cm}^2$$

Each electron produces N ions; therefore, the effective cross section $\bar{\sigma}_i$ is the average of the values at electron energy NE_i , $(N - 1)E_i$, $(N - 2)E_i$, etc. Therefore

$$\bar{\sigma}_i = 3.1 \times 10^{-17} \text{ cm}^2$$

From eq. (8)

$$p \geq 15 \text{ mTorr}$$

The smallest observed value for operation of the discharge in these experiments was 50 mTorr. It is possible, however, that the experimentally observed minimum pressure was limited by the ability to ignite the discharge at low pressures, rather than by the ability to sustain it. This question may be answered by the discharge ignition experiments to be performed during the next reporting period. Possible additional sources of discrepancy between the theory and experiment arise from the many simplifying assumptions of the theory and from the approximate nature of the physical parameters of eq. (8). However, it is important and encouraging to observe that the minimum pressure predicted for the hollow cathode discharge without magnetic field is low enough to be useful for this application.

2. Experimental Results

The first data were obtained in a magnetic field (the crossed-field hollow cathode discharge). Some of these results are shown in Fig. 19. As with the true crossed-field data described previously, the data of Fig. 19 were obtained in pulsed operation with pulsewidth of 200 μ sec and repetition frequency 10 Hz. Two important features of operation with the retracted anode were at once apparent:

1. Comparison with similar data of Figs. 12 and 13 for the crossed-field discharge indicated that the discharge voltage is somewhat higher for a given pressure and discharge current.
2. The plasma was much more difficult to ignite with the retracted anode. Ignition could not be obtained with voltages to 20 kV at helium pressures below 70 mTorr and magnetic fields up to 200 gauss. At 70 mTorr and a field of 240 G the voltage required to ignite the discharge was 6.5 kV.

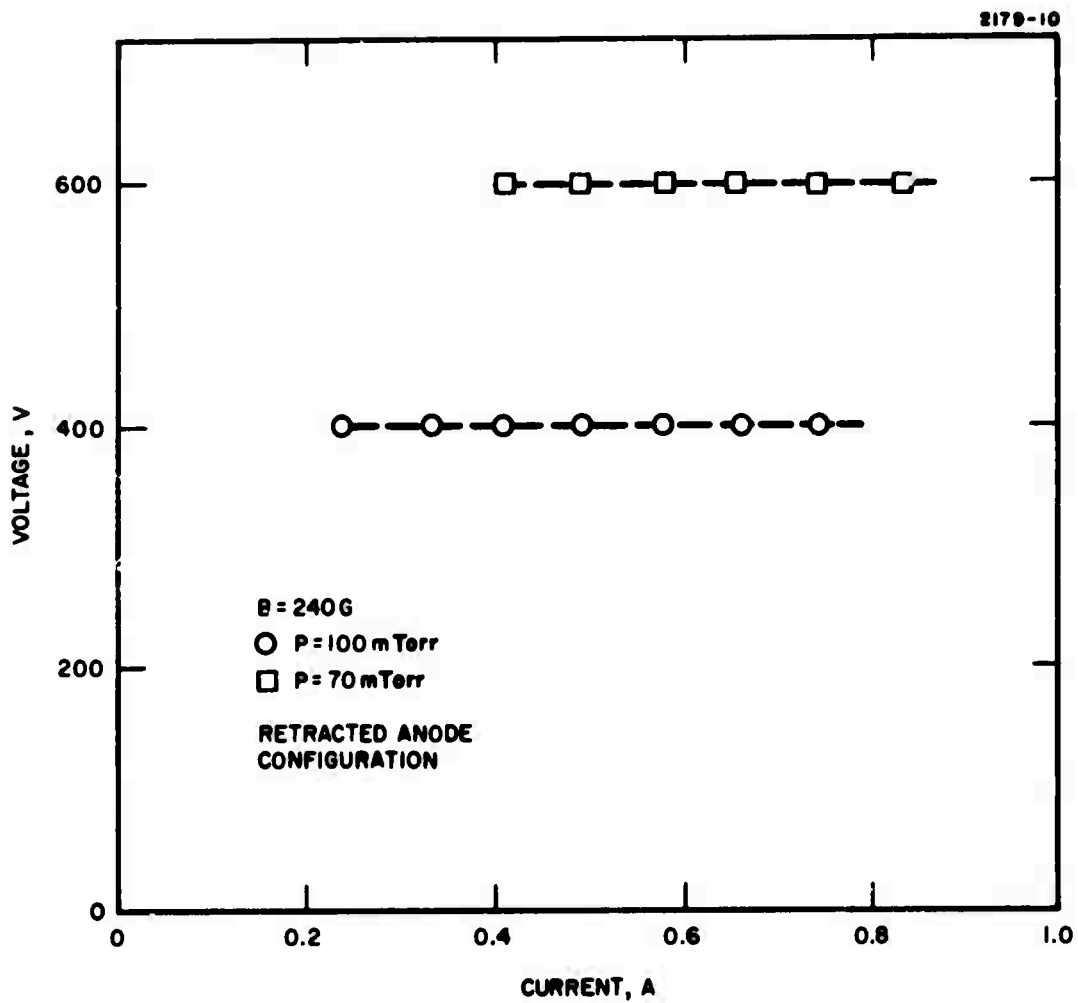


Fig. 19. Hollow cathode tube voltage-current characteristics.

Experiments were then made with a dc voltage applied to the anode. These experiments confirmed that the discharge was difficult to ignite with this electrode configuration, particularly at the low pressures (50 mTorr) at which the plasma source would have to operate in the final electron gun. The reason for the difference in ignition characteristics between the extended anode (true crossed-field) case and the retracted anode (crossed-field hollow cathode) case is that in the latter case before ignition the electric field configuration is not at all perpendicular to the magnetic field. After discharge ignition and the formation of the cathode sheath the electric field becomes more nearly perpendicular to the magnetic field and the behavior becomes qualitatively similar to the true crossed-field discharge.

To facilitate ignition at lower gas pressures a larger solenoid capable of magnetic fields to 4 kG was installed on the tube. Low pressure ignition was indeed improved at these high magnetic fields, but the discharge was observed to go into intermittent high-frequency oscillations for certain ranges of the current, pressure, and magnetic field parameters. Furthermore, on the basis of the theory outlined in Section II-B-1, it was expected that after ignition in the crossed-field mode, the hollow cathode discharge could operate without magnetic field. Hence, experiments were conducted in which the magnetic field could be removed after ignition. It was found in these experiments, as expected, that the discharge does indeed continue to operate after removal of the magnetic field, as long as the necessary voltage remains applied. Direct current operation in this fashion was necessarily restricted to low discharge currents because of possible discharge heating of the anode under dc cw conditions.

The next experimental step, which was suggested by the previous results, was to pulse the magnetic field and the applied voltage simultaneously, but with the voltage pulse lasting much longer than the magnetic field pulse. The function of the magnetic field in this case was only to facilitate ignition. The plasma was then studied in the interval following the decay of the magnetic field. A suitable low inductance

solenoid was obtained and a high current thyatron pulser assembled. It was observed that the eddy currents induced in the stainless steel cathode by the rapidly changing external magnetic field provided an effective diamagnetic shield of the plasma region for magnetic field pulses shorter than a few μsec . Measurements of the internal field were made with a magnetic probe and the length of the solenoid current pulse was adjusted to overcome the diamagnetic shielding.

Successful ignition at the desired operating pressure was achieved in this way, but the necessary ignition voltage was higher than in the dc case, approaching 20 to 30 kV at times. The operating voltage was less than 1 kV and was provided through a very large series dropping resistor. The explanation for this high ignition voltage requirement apparently concerns statistical time delay in ignition. The statistical time delay is the period between application of the discharge voltage and the appearance of an electron in the electrode gap to initiate the avalanche breakdown process. If no additional source of electrons is provided, breakdown is dependent upon initial ionization by cosmic rays. In this case the statistical time delay is about one second. The statistical time delay can always be reduced as much as desired by providing an additional electron source (a field emission point or a radioactive isotope, for example). In the dc case the time delay was unimportant since the voltage and magnetic field were applied for several seconds. In the pulsed case, however, it was necessary to reduce the statistical time delay to less than the period of the magnetic field pulse ($\sim 15 \mu\text{sec}$). The very high ignition voltage apparently accomplished this reduction by supplying additional electrons through field emission from irregularities in the cathode surface at points where the cathode-anode separation was small.

In summary, the ignition characteristics of the hollow cathode discharge at low pressure (50 mTorr) are acceptable but not very desirable for the plasma cathode electrode gun. Once the discharge is ignited, however, it appears to be a very good plasma electron source for the present application. Work on improving the plasma ignition properties of this type of discharge is continuing. At the present time an experiment

is being assembled to test a new method of ignition based upon a very thin wire ignition anode and requiring no magnetic field. Results will be reported in the Final Technical Report.

III. ELECTRON EXTRACTION

A. Theoretical Guidelines

The theoretical guidelines by which the electron extraction system operates can best be understood by reference to Fig. 20. The electron extractor consists of an electrically isolated mesh covering an aperture in the base of the hollow cathode structure. To explain the principle involved in the extractor design, the mesh is shown as two parallel wires of diameter d with center-to-center spacing h . The mesh consists of hundreds of such pairs intersected at right angles by additional pairs.

The wires as shown in Fig. 20 are biased negatively with respect to the plasma potential (which is defined to be $V = 0$). A sheath of thickness t is therefore formed at the boundary between each wire and the plasma, as shown in the figure. Since at these low gas pressures the plasma ions do not make any collisions in the sheath, the sheath thickness t obeys the following relationship

$$t^2 \propto V_s^{3/2} \quad (9)$$

where V_s is the voltage drop across the sheath. As shown in the figure, there must be an equipotential at $V = 0$ crossing the space between the wires, and this line forms the boundary between the plasma and the beam. The plasma potential is determined by the discharge anode potential in this type of discharge. If the plasma starts to "leak through" between the wires of Fig. 20 to the acceleration anode, then the plasma potential will start to rise to a value near the acceleration potential. As this happens the value V_s of eq. (9) rises, causing an increase in the sheath thickness. This decreases the size of the aperture through which plasma leakage can occur. Eventually the sheath expands to seal the aperture completely.

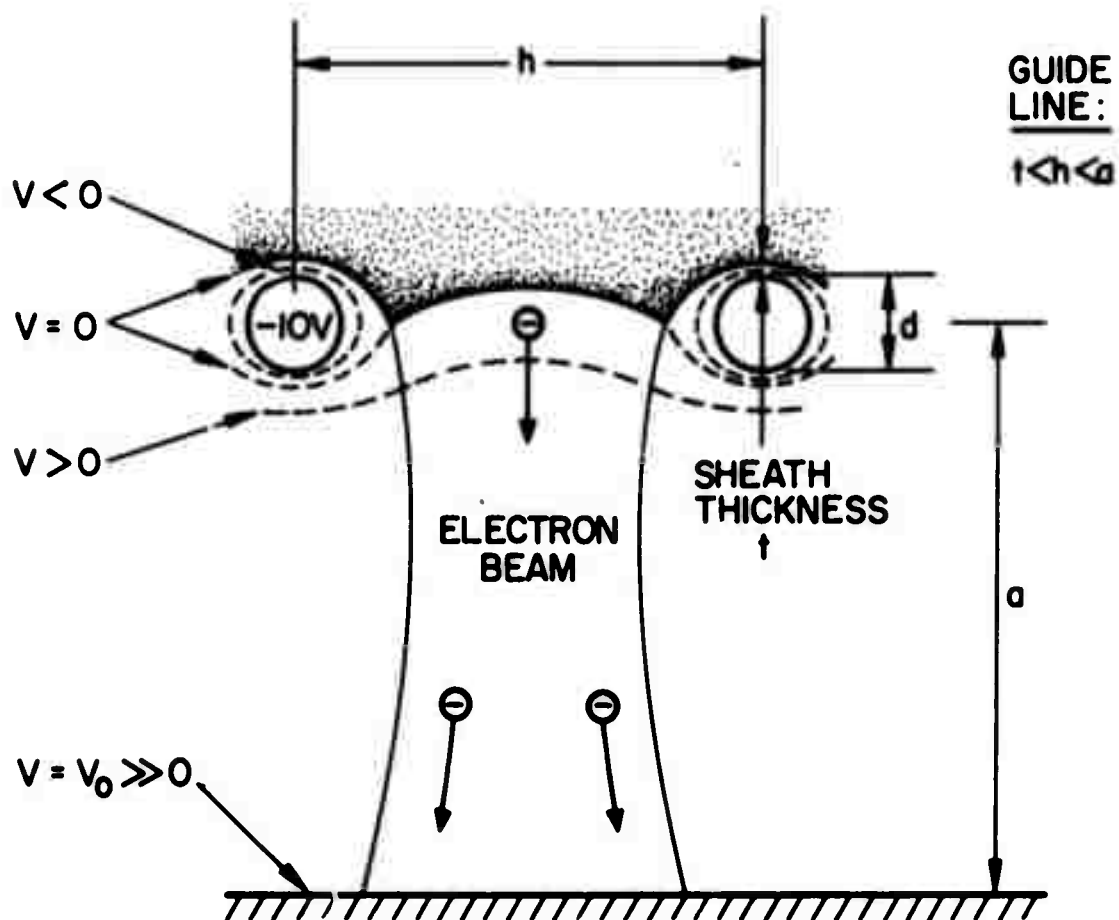


Fig. 20. Expanded view of electron extraction from plasma.

In later experiments this mesh was actually used as the anode for the hollow cathode discharge. The theoretical interpretation remains the same as shown in Fig. 21 under these conditions, the mesh potential being negative with respect to the plasma potential by an amount equal to the anode fall in the discharge. When operating in this mode the auxiliary anode was used only to ignite the discharge.

B. Experimental Results

Initial electron extraction data were obtained with the hollow cathode discharge source previously explained and the electron extractor system just described. A drawing of the extractor section is shown in Fig. 21. Three modifications were made to the cylindrical hollow cathode can to perform the electron extraction tests. First, a hole 1 cm in diameter was made in the bottom of the cylindrical can. Second, the hole was covered with a stainless steel mesh having wire diameter 0.125 mm and center-to-center spacing 0.5 mm. The mesh was electrically isolated from the cathode can and located outside the discharge region 0.5 mm from the can. Third, a solid stainless steel plate was installed parallel to and 8 mm from the mesh. The mesh served as the "extraction anode," while the plate served as the "acceleration anode." There was no control grid in this simple structure. In the rectangular high voltage gun the acceleration anode will be replaced by a control grid at the same location and the high voltage anode will be located some distance away as dictated by vacuum breakdown requirements. Pictures of the various extractor elements for the present circular geometry are shown in Fig. 22.

For these preliminary experiments it was decided to use simple resistor-capacitor decay networks wherever possible rather than building hard-tube pulzers. The quantitative behavior of the extraction system could be studied reasonably well in this way with much less cost, with much greater flexibility, and in much less time than if separate pulzers were built.

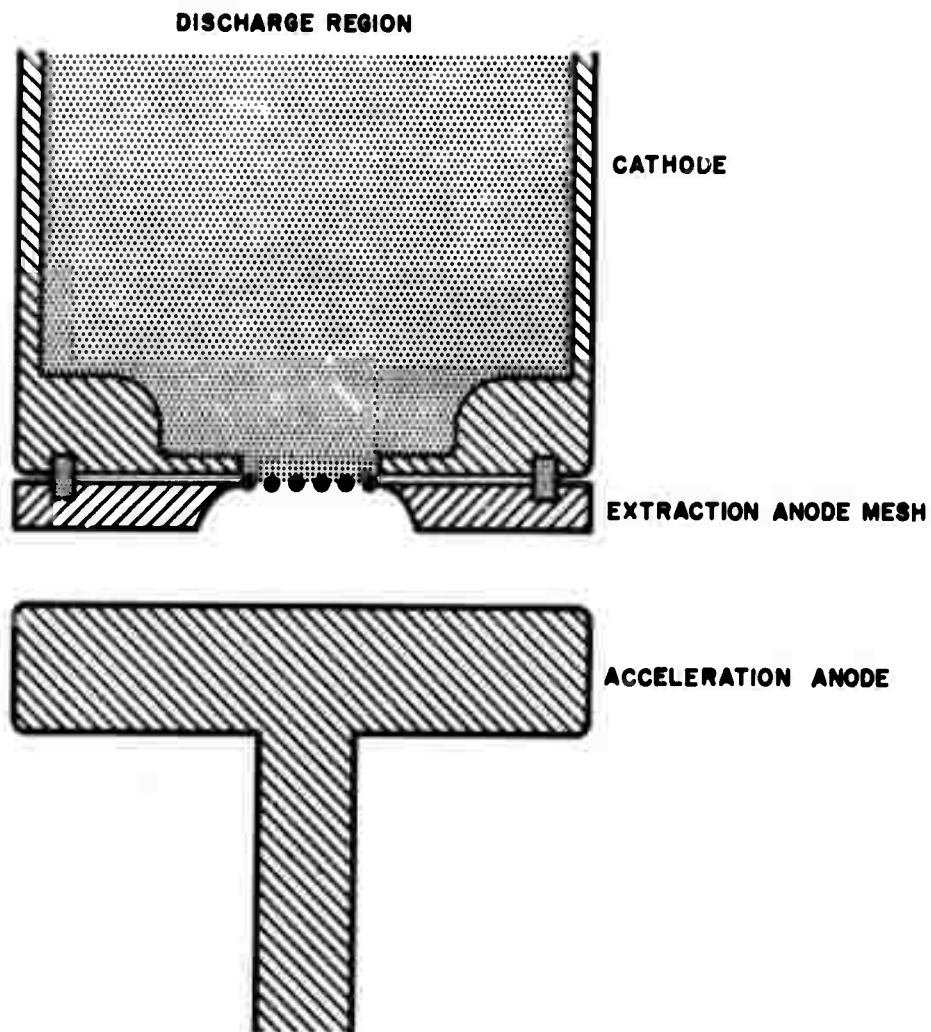


Fig. 21. Cylindrical electron extractor.

M8916

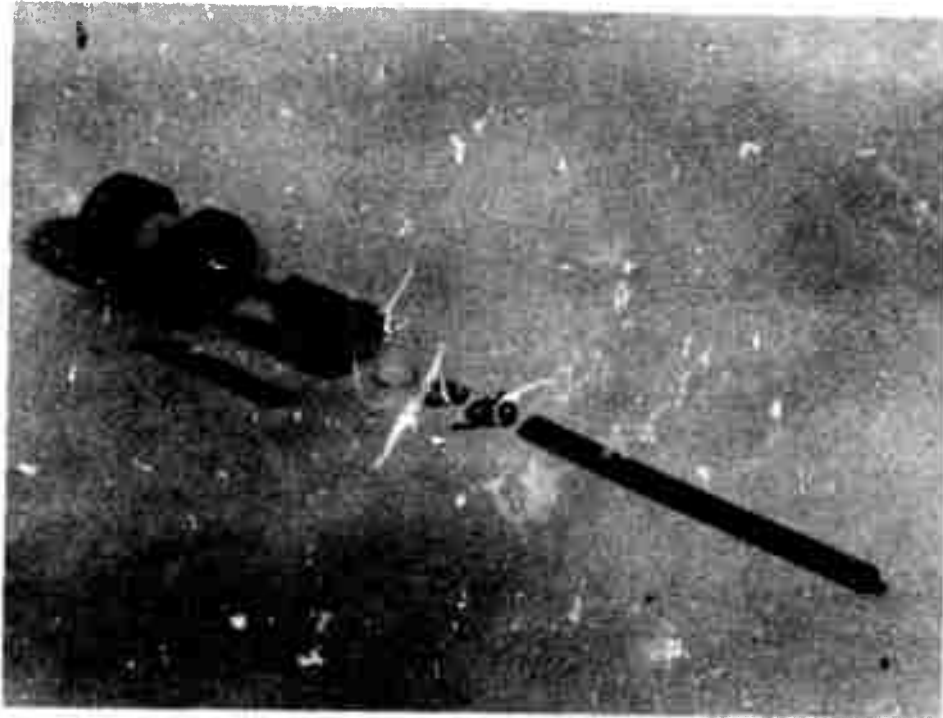


Fig. 22. Elements of cylindrical extractor assembly.

electron beams having current densities as high as 50 A/cm² have been extracted from the hollow cathode plasma electron source and accelerated to energies of 5 kV. Some of the results are given in Table I. No indication of any fundamental limit to beam current density, energy, or pulse duration was found in any of these experiments. At higher beam voltages a standoff insulator in the accelerator assembly broke down consistently; this low voltage device was designed for only 1 kV acceleration voltage.

TABLE I
Preliminary Electron Extraction Results

Pulse Length	Current Density*
1 μ sec	50 A/cm ²
10 μ sec	10 A/cm ²
75 μ sec	1.5 A/cm ²
1 msec	150 mA/cm ²
(100 μ sec)	(100 mA/cm ²)
() work statement requirement. *circuit limited.	

T760

A graph showing the general behavior of beam current density as a function of accelerator voltage is given in Fig. 23. The planar diode space-charge-limited current is also indicated as a function of voltage. The voltage of Fig. 23 is the voltage applied between the extractor and accelerator electrodes. The fact that the observed current density is greater than the space-charge limit for small

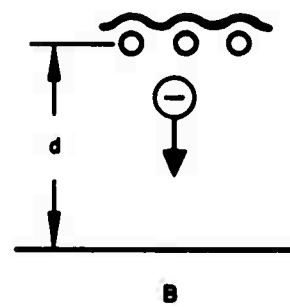
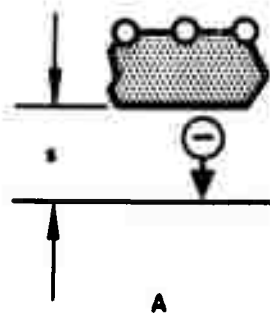
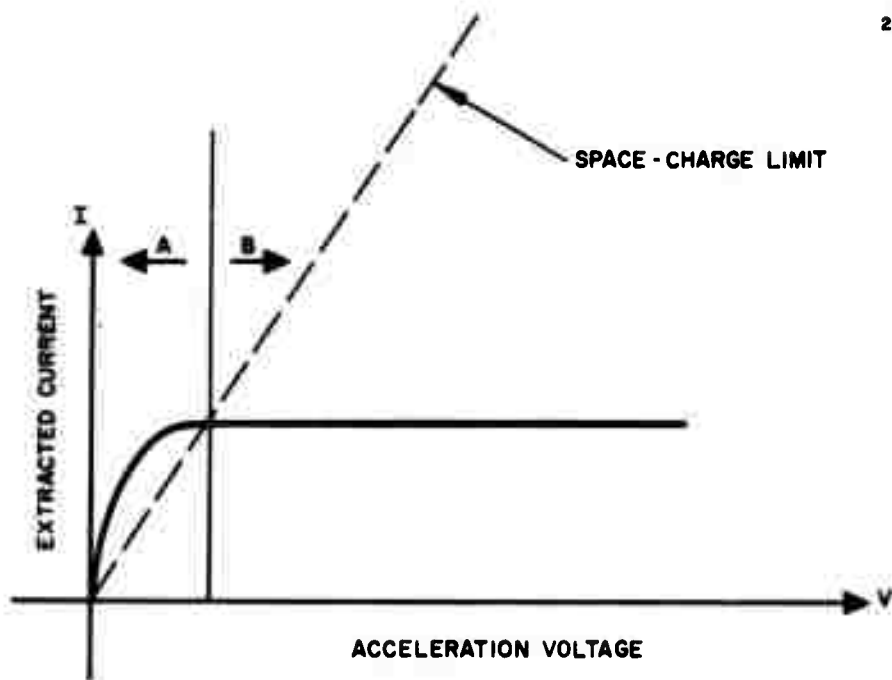


Fig. 23. Low voltage electron extraction characteristics.

acceleration voltages can be explained by a leakage of the plasma into the space between the extraction anode and the acceleration anode. A sheath is formed between these two electrodes and serves as a "virtual electrode" closer to the acceleration anode than the extractor-accelerator separation used in calculating the space-charge limited flow condition. The actual space-charge limited current from the sheath is thus greater than the calculated value. This effect occurs in region A of Fig. 23; the condition is depicted schematically in the lower left of the figure. Eventually, however, as the accelerator voltage is increased, a saturation of extracted current is reached which corresponds to the limiting current that can be supplied by the plasma. If the accelerator voltage is increased further, the sheath begins to recede from the acceleration anode until it reaches the mesh of the extraction anode. After this point is reached, additional increase in the accelerator voltage has no effect on the sheath or on the plasma conditions inside the hollow cathode source. These conditions are shown in region B of Fig. 23. The high voltage plasma cathode gun will operate in this region.

The plasma conditions inside the hollow cathode are not substantially influenced by the accelerator voltage under any conditions. They are determined essentially by the voltage differential between the hollow cathode and the mesh extraction anode, which effectively shields the cathode region from the field of the acceleration anode. As an indication of how well the cathode is shielded, the structure may be analyzed as a planar triode with the extraction anode as the triode grid. The resulting amplification factor μ is approximately 1000, indicating that the effect on the cathode current of the "grid" (extraction anode) voltage is 1000 times greater than the effect of the accelerator voltage. Experimentally, no change in cathode current is observed when the accelerator voltage is changed from 0 to 5 kV, its present upper limit determined by insulator breakdown. With no voltage applied to the accelerator, all of the cathode current

goes to the extraction anode. As the accelerator voltage is increased from zero the cathode current divides, part (the extracted beam current) going to the acceleration anode and part to the extraction anode. The total cathode current remains unchanged, however. At higher acceleration voltages the extracted beam current continues to increase and finally saturates at a value approximately equal to the hollow cathode current. At this point the current to the extraction anode is very small.

These two features of operation of the present device strongly suggest that at high accelerator voltages there is no discharge in the accelerator region. First, the saturation of extracted current as the voltage between the extractor and accelerator is inconsistent with the existence of a discharge in this region. Second, the complete independence of the plasma conditions in the source from the accelerator voltage would not be expected if a discharge to the accelerator were occurring. Both these features are suggestive that ionization in the acceleration region is minimal and that the extracted electron beam reaches the acceleration anode with full beam energy equal to the voltage applied to the accelerator.

IV. PASCHEN BREAKDOWN

A. Effect of High Voltage Beam on Breakdown Characteristics

As discussed in Section I, Paschen breakdown is simply the usual form of electrical breakdown associated with gas discharge devices. It begins as an ionization avalanche process in which an electron in the gap between the electrodes is accelerated by the applied field, making ionizing collisions with neutral gas atoms. The resulting secondary electrons are also accelerated and ionize additional atoms, creating the avalanche process.

If the electrodes are irregularly shaped and the resulting spacing between them is variable, Paschen breakdown can occur either between the most widely separated points on the electrodes or between the most closely spaced points, depending on the experimental conditions. In helium, for example, with electrode spacings greater than 1 cm and gas pressures greater than a few Torr, breakdown occurs at moderate voltages between the most closely spaced points on the electrodes. At much lower pressures breakdown occurs between the most widely separated points. The physical reason for this behavior is that at moderate gas pressures the mean free path for ionization is much shorter than the electrode gap. Thus for moderate voltages the ionization probability is highest where the applied field is largest, i.e., where the electrode gap is smallest, and this is where breakdown occurs. At very low pressures, however, the mean free path for ionization becomes longer than the closest electrode spacing. No ionization can then occur in this region, and the breakdown occurs at the point of widest separation of the electrodes.

Paschen breakdown behavior may be well represented by a Paschen curve shown schematically in Fig. 24. The abscissa is the product of (pressure) \times (electrode spacing) pd in cm-Torr. The ordinate shows the breakdown voltage as a function of the pd product. In region II to the right of the Paschen minimum, for a given gas pressure and electrode configuration, as the applied voltage is

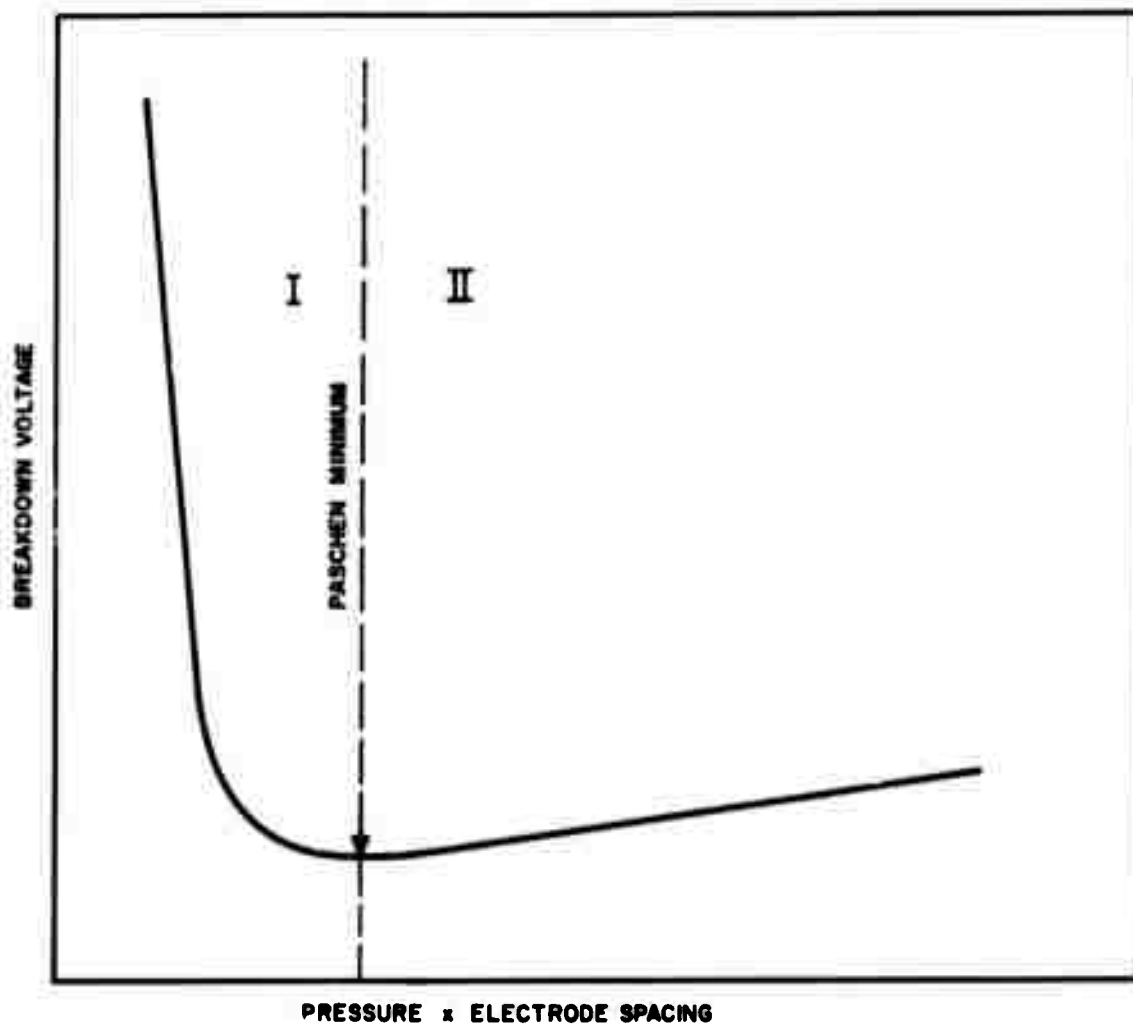


Fig. 24. Qualitative behavior of Paschen breakdown voltage as a function of pressure x electrode spacing.

increased breakdown occurs between the closest points of the electrode system (minimum pd). In region I, however, to the left of the Paschen minimum as the applied voltage is increased breakdown occurs between the most widely separated electrode points (maximum pd). A typical discharge tube electrode system represents a range of pd values determined by the operating pressure and the minimum and maximum electrode separations of the system. This range of values determines whether the system is operating in region I or region II of Fig. 24.

The region to the right of the Paschen minimum in Fig. 24, region II, is of no interest for the plasma cathode electron gun, because in this region as soon as electrons gain energy equal to the energy of peak ionization efficiency, breakdown occurs and no additional increase in electron energy occurs. Operation to the left of the Paschen minimum, in region I of Fig. 24, however, allows the acceleration of electrons to very high energies without breakdown. The physical reason for this ability to accelerate high-energy electrons without breakdown is that the electrode separation, which determines the length of the acceleration path, is so short compared with the ionization mean free path that ionizations by electron impact are improbable and the avalanche process described earlier cannot develop.

Considerable data on Paschen breakdown in helium to the left of the Paschen minimum exist in the scientific literature. Some of these data are shown in Fig. 2. In all cases, the data were obtained by applying a uniform field to a gas between parallel plate electrodes and recording the breakdown voltage. These results are not adequate for the present application, however, because (1) the observed discrepancies in the data are rather large, and (2) the observed breakdown characteristics give no experimental information on the possible effect of a high energy electron beam on breakdown. Although the theory of Paschen breakdown indicates that a high energy electron beam should not affect breakdown, the importance of this question motivated an experimental investigation.

Since the operation of the plasma cathode electron gun relies on the ability to accelerate the electrons through a low pressure gas without Paschen breakdown, it was decided to investigate the Paschen breakdown characteristics of helium in the presence of an electron beam. The test apparatus was designed to resemble the acceleration section of the high voltage plasma cathode e-gun so that the results would be most directly applicable to the design of this device. In addition, by turning off the electron beam the device could be used to obtain additional values for the data of Fig. 2.

A sketch of the assembled experimental device is shown in Fig. 25. The test vehicle consists of two parallel circular stainless steel electrodes enclosed in a ceramic vacuum envelope. A 1 mm diameter hole is located in the center of the negative electrode, and directly behind the hole, also in vacuum, is a simple tantalum strip thermionic cathode. The unit should withstand a maximum applied voltage of several hundred kV, but it will be tested only to 150 kV during this program. The device has just been assembled on a vacuum pumpout and gas filling station. Data will be obtained at the beginning of the next reporting period.

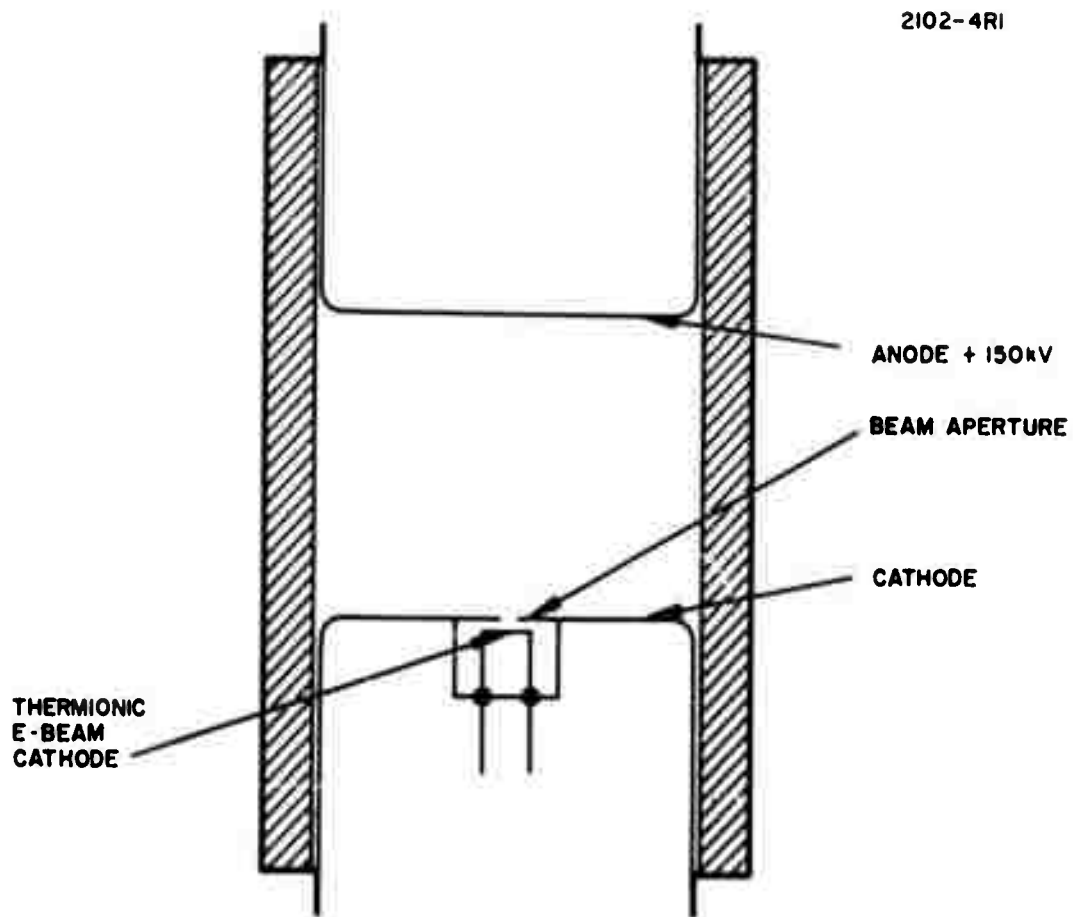


Fig. 25. Assembly for study or Paschen breakdown in the presence of E-beam.

V. DESIGN OF HIGH VOLTAGE PLASMA CATHODE ELECTRON GUN

A. Basic Design Parameters

With experience gained from the low voltage circular plasma cathode electron gun described in Sections II and III, a large scale, high voltage rectangular gun has been designed, and fabrication of various subassemblies is now in progress. ~~The following parameters~~ of this gun are specified in the work statement of this contract:

Minimum beam dimensions 1 cm x 10 cm

Minimum current density 100 mA/cm²

Minimum beam voltage 150 kV

Minimum pulse duration 100 μ sec

The low voltage electron extraction experiments indicate that the beam current density and pulse duration probably can be extended well beyond these minimum values. The beam dimensions also have been set somewhat higher than the minimum at 1 cm x 13 cm at the exit plane from the plasma source.

The remaining beam parameter, the voltage, is critically determined by the spacing of the high voltage accelerator electrodes and by the delicate balance between vacuum breakdown and Paschen breakdown. If we take from Fig. 2 the data for Paschen breakdown, and if we conservatively estimate that the rectangular plasma source for this gun will operate well at a helium pressure of 50 mTorr, based on our experience with the smaller cylindrical plasma source, we can plot the Paschen breakdown voltage as a function of the accelerator electrode spacing, as in Fig. 26. In addition, experience in this laboratory and others has shown that a conservative limit for vacuum breakdown is an applied field on the order of 70 kV/cm between flat polished stainless steel electrodes. We can therefore indicate on Fig. 26 the voltage for vacuum breakdown as a function of electrode separation.

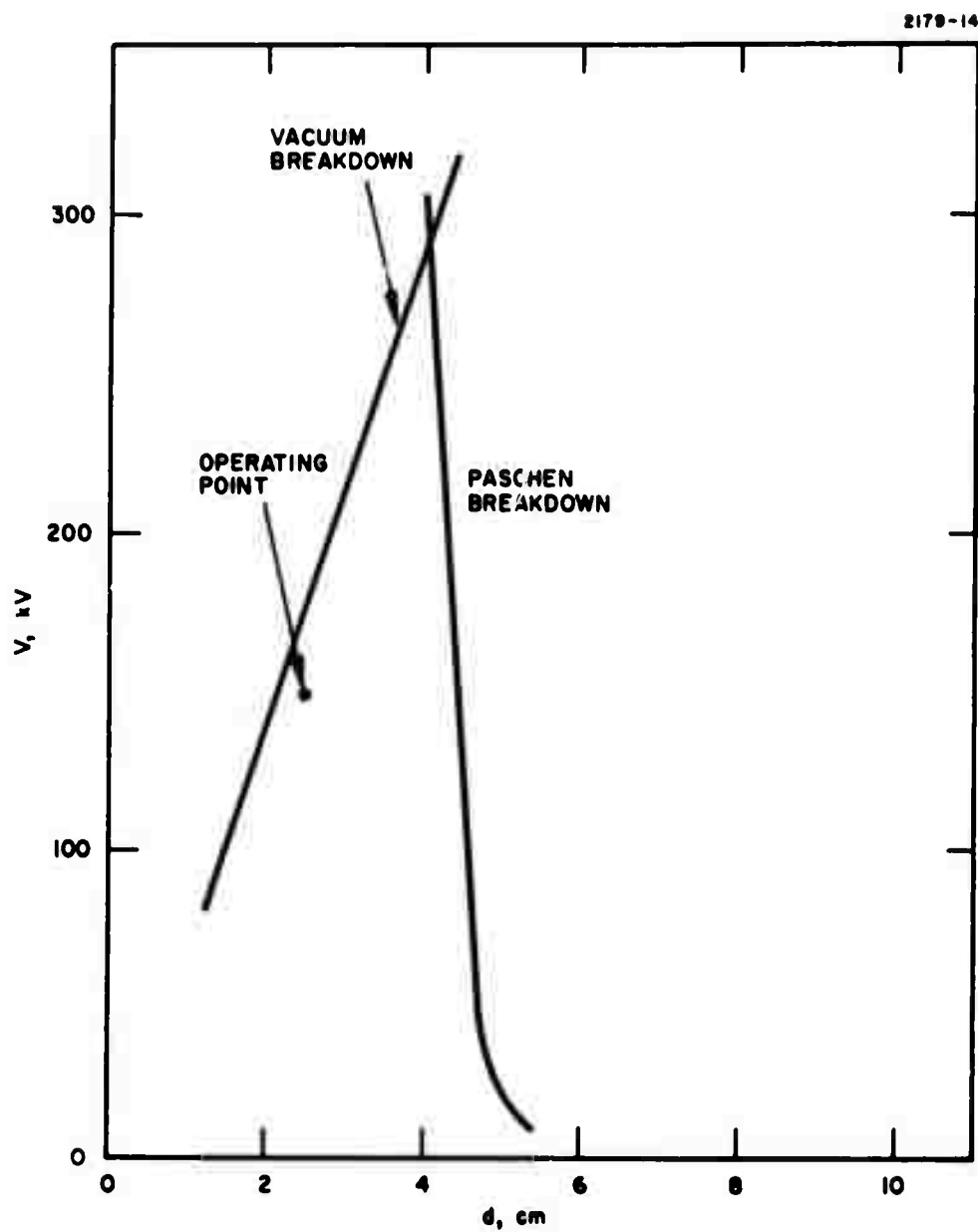


Fig. 26. Operating point of high-voltage rectangular gun in relation to vacuum and Paschen breakdown.

Thus the two breakdown limits are clearly seen in the figure, and the theoretical maximum operating voltage at a pressure of 50 mTorr is ≈ 290 kV, which would be achieved with a design electrode spacing of 4.2 cm. It should be noted, however, that the curve of Fig. 26 indicating Paschen breakdown may shift to the left or right as firmer data become available from our own experiments. In addition, the Paschen breakdown curve will shift to the left or right as the operating helium pressure of the tube is raised or lowered. The vacuum breakdown curve, however, is well known and rather firmly fixed at 70 kV/cm. Because of the relative uncertainties in the Paschen data it was decided to fix the operating point of the tube as far as possible from the Paschen limit, which puts the point very close to the vacuum breakdown limit. An electrode spacing of 2.5 cm has been chosen for the initial tests. This definitely limits the maximum operating voltage of the gun to 175 kV. If tests show that the Paschen breakdown limit is far to the right of that shown in the figure, the electrode separation can easily be increased to provide a higher safety margin against vacuum breakdown.

B. Design of Rectangular Gun

A drawing of the full size rectangular gun is shown in Fig. 27. It will be enclosed by a cylindrical ceramic vacuum envelope, shown in Fig. 28, which will also serve as the high voltage insulator. Electron extraction into the acceleration region will be through a rectangular mesh as shown. The mesh shown, which is located flush with the negative electrode, is actually a control grid, which will allow regulation of the beam independent of the plasma electron source or accelerator voltage. The plasma electron source will be essentially a rectangular version of the circular source used successfully in the low voltage experiments. A cross-sectional view of the device is shown in Fig. 29. Parts for this gun are presently being fabricated. Assembly is scheduled to begin shortly, and operation and evaluation of the device will take place in the next reporting period.

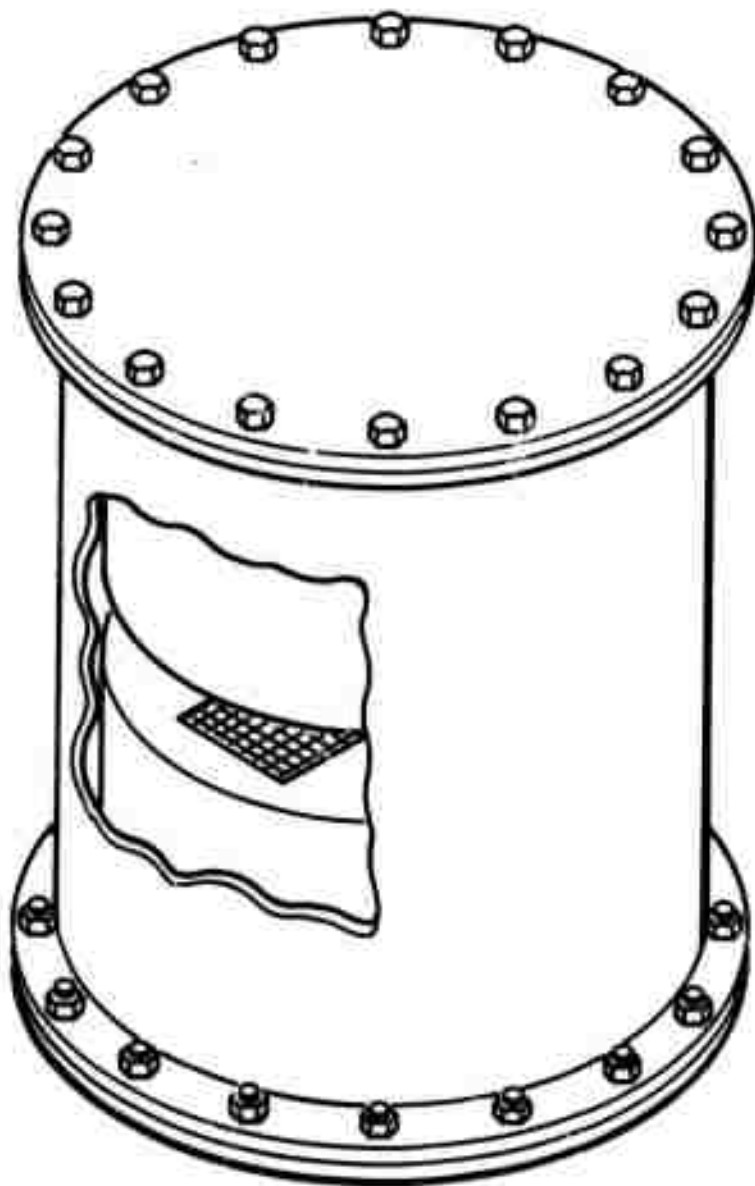


Fig. 27. Artist's drawing of high voltage plasma cathode electron gun without corona shielding.

M9204

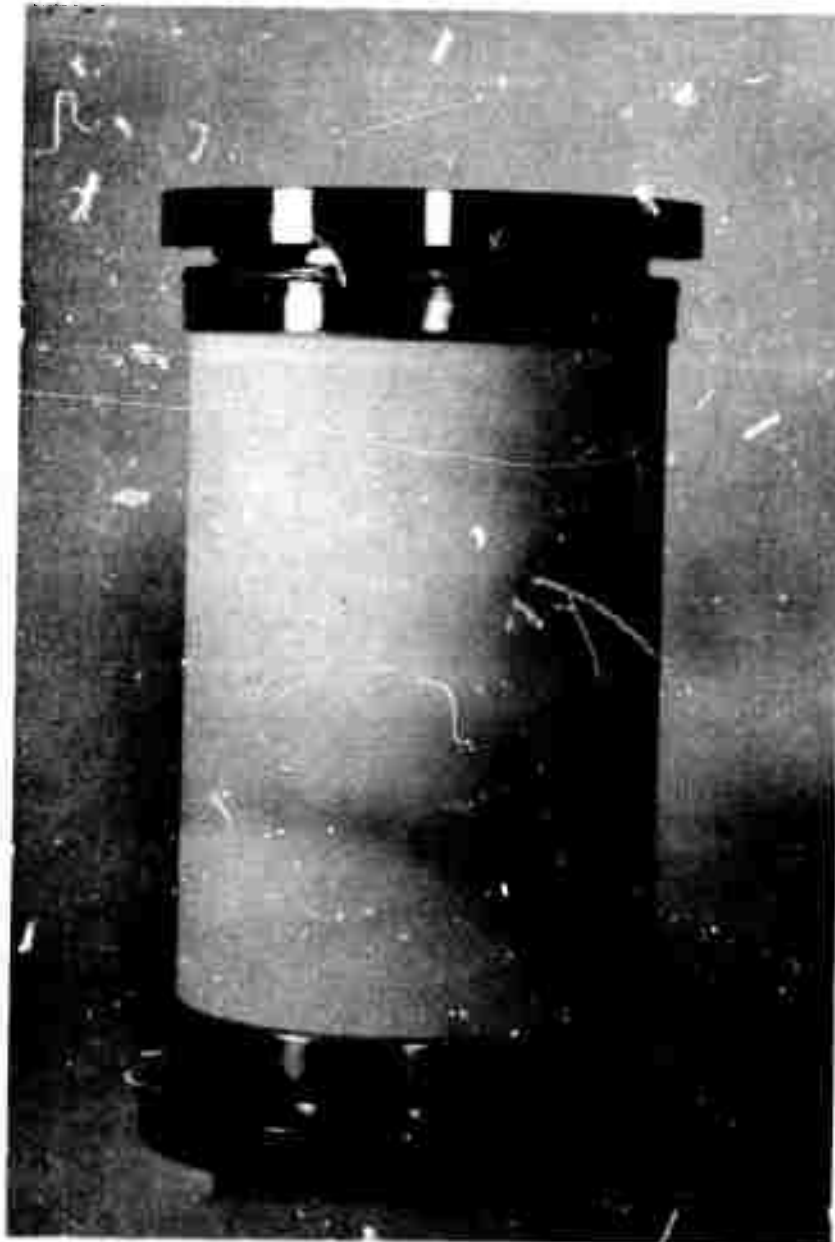


Fig. 28. Ceramic vacuum envelope and insulator for high-voltage rectangular gun.

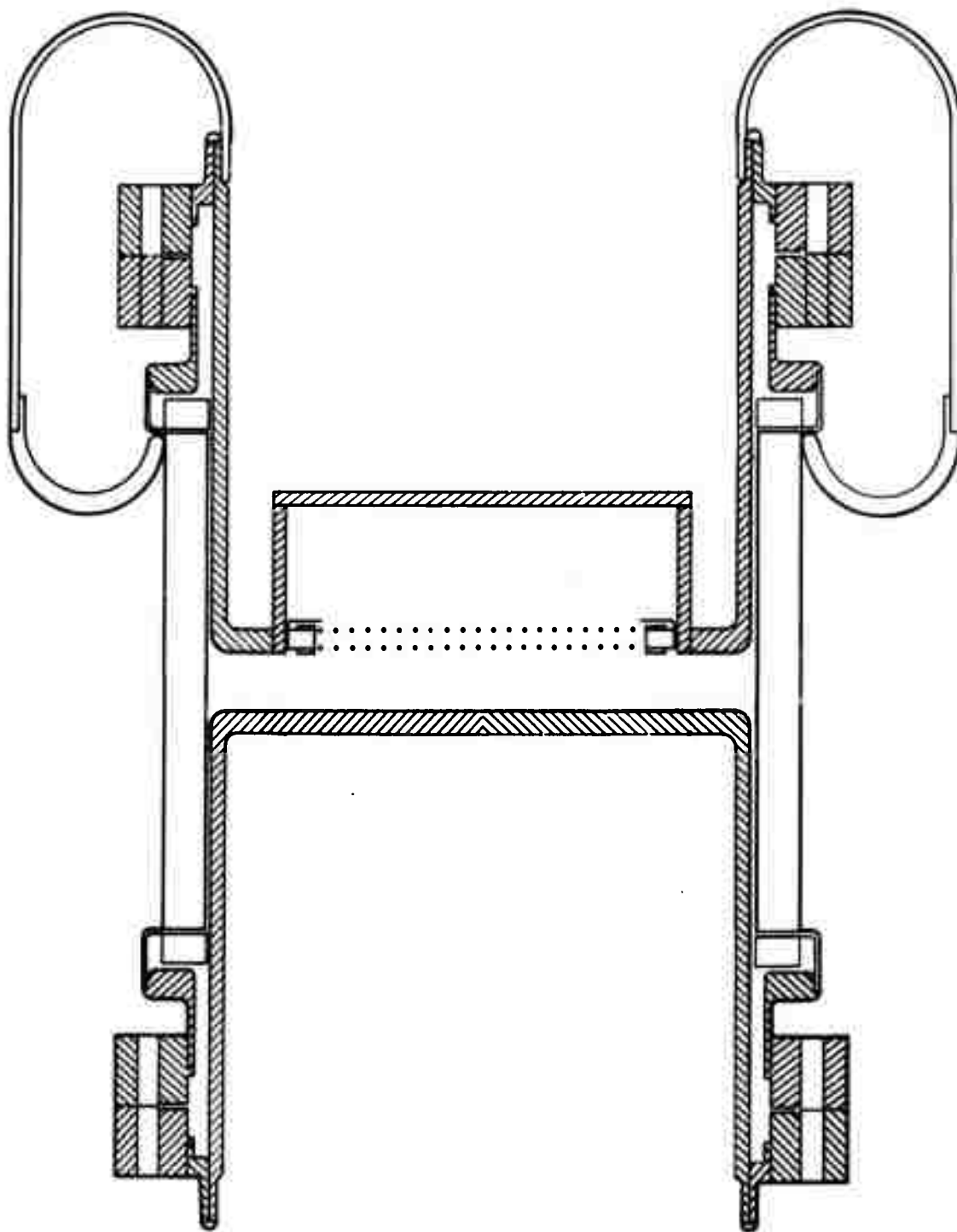


Fig. 29. Cross-sectional schematic of high-voltage rectangular gun.

VI. CONCLUSIONS AND FUTURE PLANS

The work of the first half-year of this program has experimentally established the validity of the plasma cathode concept. It is expected that an electron beam meeting all of the goals outlined in Section I-A will be produced during the current program. A plasma source operating at low gas pressures has been developed and tested successfully. A method of electron beam extraction from the plasma and subsequent acceleration has been devised and tested. Beam current densities as high as 50 A/cm^2 have been produced. This value is well in excess of the program goal of 100 mA/cm^2 . At lower current densities (150 mA/cm^2) pulse durations of 1 msec have been observed. This pulse length also comfortably exceeds the program goal, which is $100 \mu\text{sec}$.

The results obtained to date have been encouraging. Effort during the remaining two months of the current program will be concentrated on meeting the remaining program goals for beam dimensions and energy. The following specific tasks will be undertaken.

1. Investigation of new plasma ignition methods designed to make the plasma cathode simpler and more reliable.
2. Measurement of Paschen breakdown characteristics in the presence of a high energy electron beam. The results of this measurement will provide additional information for the design of the accelerator section of the high voltage device. The present accelerator design is based on Paschen breakdown data without an electron beam, and if the results of the measurement confirm theoretical expectations, no design change will be necessary.
3. Continuation of fabrication of high voltage rectangular device. This device, which will produce an electron beam meeting all the program goals, will be tested and optimized as the final task of the current program.

REFERENCES

1. R.K. Garnsworthy, L.E.S. Mathias, and C.H.H. Carmichael, Appl. Phys. Letters 19, 506 (1971).
2. The Glow Discharge at Low Pressure, by Gordon Francis, in Handbook of Physics 22, edited by S. Flügge.
3. L.G. Guseva, Sov. Phys. - Tech. Phys. 15, 1760 (1971).
4. D.D. Aleksandrov, N.F. Olendzkaia, and S.V. Ptitsyn, Sov. Phys. - Tech. Phys. 3, 836 (1958).
5. R. Quinn, Phys. Rev. 55, 482 (1937).
6. G.A. Hofmann, Hughes Research Laboratories Research Report No. 420 (1970).
7. L.L. Alston, High Voltage Technology (Oxford University Press, London, 1968).
8. Sanborn C. Brown, Introduction to Electrical Discharges in Gases (Wiley, 1966).
9. Karl R. Spangenberg, Vacuum Tubes (McGraw-Hill, 1948).